Pergamon

Geochimica et Cosmochimica Acta, Vol. 59, No. 9, pp. 1669–1697, 1995

0016-7037/95 $9.50 + .00

0016-7037(95)00075-5

The albite-water system: Part II. The time-evolution of the stoichiometry of dissolution as a function of pH at 100, 200, and 300°C

ROLAND HELLMANN[1,2,*]

[1]Laboratoire de Géochimie, U.R.A. 067 C.N.R.S., Université Paul Sabatier, 38, rue des Trente-Six Ponts, 31400 Toulouse, France
[2]Crustal Fluids Group, L.G.I.T.-I.R.I.G.M., BP 53X, Université J. Fourier, C.N.R.S., Observatoire de Grenoble, 38041 Grenoble Cedex, France

(*Received June* 21, 1994; *accepted in revised form January* 28, 1995)

Abstract—Albite feldspar was hydrolyzed over a wide-range of pH conditions at 100, 200, and 300°C. The release rates of Na, Al, and Si were measured as a function of time from the initial, pre-steady-state phase to the attainment of steady-state, congruent dissolution conditions. Leached layers were developed during the initial stages of dissolution due to the preferential release of Na with respect to Al and Si at nearly all pH and temperature conditions. The preferential release of Na is due to the higher rate of ion exchange reactions vs. hydrolysis reactions associated with the release of Si and Al. The depths of Na preferential leaching show a pH dependence. Maximum depths on the order of 1500 and 1200 Å were recorded at acid and basic pH conditions, respectively, whereas minimum depths were observed in the neutral pH range. Leached layers deficient in Al (with respect to Si) were recorded at acid and neutral pH conditions. At mildly basic pH conditions, Al and Si were congruently released, or alternatively, either Al or Si was preferentially released. At more extreme basic pH conditions, only Al was preferentially released. The depths of Al preferential leaching were not determinable under all conditions due to the precipitation of an Al surface phase; a maximum recorded depth of 250 Å was determined at basic pH conditions. The preferential release behavior of Al and Si is ascribed to the pH dependency of the speciation of Al-OH and Si-OH groups at the surface and within the leached layers. However, at very basic pH conditions, where $Al\text{-}O^-$ and $Si\text{-}O^-$ groups are postulated to predominate, the preferential release of Al is probably due to the intrinsically greater reactivity of Al-bridging oxygen bonds.

Calculations of diffusion coefficients for Na diffusion within the leached layers suggest that leached layers are structurally more open and porous than unaltered, crystalline albite. In addition, the calculated diffusion coefficients show a strong pH dependence. This result implies that leached layers formed at acid and basic pH conditions undergo a greater degree of structural modification since they are more open than those formed at neutral pH. The pH-dependent nature of the structural and transport properties of leached layers can be considered to be a contributing factor to the overall pH dependence of feldspar dissolution rates.

The formation of leached layers is an important factor in providing hydrolyzing molecules (H^+, H_2O, OH^-) access to Na^+ exchange sites and Si-O-Si and Al-O-Si hydrolysis sites deep within the structure. Evidence for this is shown by the positive relationship between the overall rates of dissolution and the depths of Na and Al leaching. The data from this study suggest that reactions at the surface and within leached layers control the overall dissolution behavior of feldspars and other similar, multi-oxide silicates. It is therefore proposed that a "leached layer-surface reaction" model more accurately describes the dissolution process at elevated temperatures than the traditionally accepted "surface reaction" model.

INTRODUCTION

Despite numerous geochemical studies devoted to feldspar-water interactions, much still remains to be learned about the exact nature of the dissolution process. To date, most of the theories on the mechanisms of feldspar dissolution have been based on work carried out at low temperatures, which in the majority of cases has been at 25°C. However, with the exception of chemical weathering reactions at the Earth's surface, most mineral-water reactions take place in subsurface crustal environments, where temperatures can range into the hundreds of degrees. It has thus become necessary to question whether our present assumptions on the mechanisms of feldspar dissolution are also valid at elevated temperatures.

With this in mind, a systematic study of the stoichiometry of albite feldspar dissolution at hydrothermal conditions was conducted. The experiments were carried out at 100, 200, and 300°C over a wide range of pH (1.3–10.3) conditions. The span in experimental pH, obviously being much larger than that which might occur under natural conditions, was chosen to ensure a better quantification of the effect of pH on the stoichiometry and mechanisms of dissolution. This study is the second in a series devoted to the albite-water system at elevated temperatures. A previously published article on the steady-state dissolution kinetics of albite, at the same experimental conditions as cited above (Hellmann, 1994), will henceforth be referred to as Part I.

The main purpose of the present study is to document the changes in the stoichiometry of dissolution as a function of time for each particular set of dissolution conditions. The time evolution of the stoichiometry is based on the aqueous release rates of Na, Al, and Si that are measured from the initial stages

* *Present address:* Crustal Fluids Group, L.G.I.T.-I.R.I.G.M., BP 53X, Université J. Fourier, C.N.R.S., Observatoire de Grenoble, 38041 Grenoble Cedex, France.

of dissolution (i.e., non-steady-state behavior) to the establishment of steady-state conditions. Elemental release rates contain information on how a particular element in a mineral structure interacts both with the hydrolyzing molecules of an aqueous solution and with the other elemental constituents of the solid. This is necessary for obtaining information on the detailed nature of the dissolution process, which in the case of feldspars and similar multiple oxides, is very complex and is thought to consist of the following steps: ion-exchange reactions on the surface and within the structure, diffusion of solvent molecules into the structure and their subsequent adsorption at hydrolysis sites, hydrolysis of framework bonds and subsequent detachment, outward diffusion of hydrolysis products through the structure, and potential precipitation of secondary phases on the surface, as well as possible direct formation of secondary phases within the hydrolyzed near-surface region (see Casey et al., 1993).

Elemental release rates contain information on how these individual processes are coupled with one another; they can also provide a means for estimating which one is rate-limiting. Their utility becomes particularly apparent when it is the initial, transient stages of nonstoichiometric dissolution that are being studied. In addition, release rates provide information for determining which element is best suited, and under which particular conditions, for use in formulating an overall dissolution rate (i.e., avoidance of those elements that tend to precipitate, adsorb on surfaces, etc.). The form of an overall rate law, of course, also depends on the type of physical or chemical process that is rate limiting.

When specifically considering feldspar dissolution, two general models for dissolution have been proposed in the literature. The first proposes that the overall dissolution rate is limited by diffusion; the second is based on the rate being limited by surface chemical reactions. The relative importance of these two processes during dissolution has been the basis of long debate. The applicability of these two models to feldspar and other aluminosilicate dissolution reactions has been described in the geochemical literature for nearly three decades now (for more details see Holdren and Berner, 1979; Chou and Wollast, 1984).

Feldspars often display incongruent dissolution behavior, where the degree of incongruency depends on such factors as solution pH, temperature, and composition. Under some conditions, most notably at neutral pH and room temperature, leached layers are negligibly small (Chou and Wollast, 1984). Under acidic pH conditions, the initial stages of dissolution are marked by a rapid (on the order of minutes) ion exchange process (Garrels and Howard, 1957; Chou and Wollast, 1985a), where alkalis in the surface structure are exchanged with protons in the solvent solution. At basic pH, positively charged species in the solution are exchanged with alkalis (see results in Hellmann et al., 1990). Evidence for ion exchange has also been shown by the anticorrelation of Na and H profiles in the near surface of hydrolyzed albite using a resonant nuclear reaction analysis (RNRA) ion beam technique (Petit et al., 1990). The initial incongruent stage of dissolution due to ion exchange reactions is then followed by a much longer period of dissolution (minutes to several hours, depending on the experimental conditions) that is characterized by the preferential release of certain framework elements (Correns and von Engelhardt, 1938; Chou and Wollast, 1984; Holdren and Speyer, 1985; Casey et al., 1988; Hellmann et al., 1990). Eventually, steady-state conditions of dissolution are attained, such that all elements are released at stoichiometrically equal rates. The sequential stages of the dissolution process described above have been extensively studied using batch-type reactors. The results have been described in the literature in terms of concentration vs. time curves that show a change from exponential, to parabolic, to linear behavior (see Busenberg and Clemency, 1976; Fung et al., 1980).

The observation that feldspars can dissolve incongruently during the initial stages of dissolution led researchers to postulate that surface or near-surface layers, with a composition different from that of the bulk, must develop. The diffusion model is based on the premise that these surface layers diffusionally-limit the overall dissolution process. The exponential and parabolic kinetics that were observed in batch-type experiments could then be explained in terms of the growth of such a layer, where the inward diffusion of reactants and/or the outward diffusion of hydrolysis products through this layer control the overall rate of dissolution. The exact nature of this layer has been subject to debate.

One interpretation of the layer is based on the precipitation of either an amorphous gel or a crystalline phase (Wollast, 1967; Helgeson, 1971, 1972). Even though surface precipitates have been documented, there has never been proof that they affect the outward diffusion of species (see Hellmann et al., 1989, for example). Velbel (1993) recently showed that surface precipitates are not diffusionally inhibiting unless the molar volume ratio of product (the precipitate) to reactant is greater than one. An alternative interpretation is based on the preferential release of elements leading to the formation of leached layers within the near surface. Based on a feedback model, the leached zone increases in thickness up to a point where the outward flux of diffusionally limited hydrolysis products (i.e., those elements which are preferentially released) becomes equal to the rate of retreat of the outer boundary of the leached layer (the rate of release of residual framework element(s) at the surface/fluid interface) (Correns and von Engelhardt, 1938; Luce et al., 1972; Pačes, 1973; Busenberg and Clemency, 1976; Tsuzuki and Suzuki, 1980; Chou and Wollast, 1984, 1985a).

The diffusion model has been challenged on several fronts. Lagache (1965) was among the first to point out that the intrinsic rate of feldspar dissolution was a linear function of time (for dissolution in a batch reactor), and that deviations from this behavior were due to precipitation reactions that were distinct and not coupled to the overall dissolution rate (see also Petrović et al., 1976; Busenberg, 1978; Holdren and Adams, 1982). Linear kinetics of dissolution thus became synonymous with a surface reaction model, where steady-state dissolution is congruent and the reaction rate is proportional to the surface area and independent of time. Various theoretical models of surface reaction dissolution have been advanced in accord with this model, such as those based on transition state theory and the breakdown of activated surface complexes (Aagaard and Helgeson, 1982) and on the rate of detachment of product species at step and kink sites (Dibble and Tiller, 1981). SEM images of reacted surfaces, showing etch pits that formed at surface sites with excess energy (dislocations, twin boundaries, etc.), offer experimental evidence in support of the surface reaction model (Berner and Holdren,

1979). Berner and Holdren (1979) also examined naturally weathered feldspar soil grains with X-ray photoelectron spectroscopy (XPS) and found no evidence for any significant leached layers with a composition different from that of the bulk. Explanations for initial nonlinear dissolution behavior, in the absence of precipitates, were based on the dissolution of ultrafine surface particles (Holdren and Berner, 1979) or on the dissolution of a mechanically disturbed surface layer (Petrovich, 1981a,b).

Nonetheless, based on recent experiments using grains with well-conditioned surfaces (i.e., absence of surface fines, predissolution of any mechanically strained surface layers) and run under experimental conditions that precluded the precipitation of secondary phases, there is generally still conclusive evidence for initially incongruent dissolution, and by implication, the existence of leached layers (Schweda, 1990; Stillings and Brantley, 1995). The thickness of the surface layers has been found to be a function of solution composition (Chou and Wollast, 1984, 1985a) and solution pH (Holdren and Speyer, 1985). Definitive proof for the existence of leached layers, up to several thousand Å in thickness, has been revealed over the last decade by the application of several spectroscopic (XPS, Auger) and ion beam techniques (RNRA, RBS, ERDA, SIMS) to the study of surface and near surface regions of hydrolyzed feldspars and other silicates (Petit et al., 1987, 1990; Casey et al., 1988, 1989; Hochella et al., 1988; Muir et al., 1989, 1990; Hellmann et al., 1990). The sample surfaces examined by XPS by Berner and Holdren (1979) were probably weathered at close to neutral pH conditions, where leached layers are generally negligible, with thicknesses not exceeding a few tens of Å. It should be noted that even at 225°C, the dissolution of albite in deionized water led to the development of leached layers only 10–20 Å thick (Hellmann et al., 1990).

From the evidence discussed above, it is obvious that aspects of both models are not mutually exclusive, as was pointed out by Chou and Wollast (1985b). It is, however, also apparent that both theories, taken by themselves, do not accurately describe the complete dissolution process from $t = 0$ to $t \rightarrow \infty$. A more complete understanding of the dissolution behavior of complex minerals, such as feldspars, requires a different model altogether. An attempt to reconcile this problem calls for a "leached layer-surface reaction" model that specifically considers the formation of leached layers and their influence on the overall reaction kinetics of dissolution. Thus, in this model, reactions that occur within leached layers are postulated to influence the rates of bond breakage and the subsequent release of both network-modifying elements (alkalis) and network-forming elements. It is also important to note that aspects of both previous models, surface reactions and the diffusion of species through leached layers, are an integral part of this model.

One of the primary purposes of this study is to present results that detail the formation of leached layers, based on the time evolution of the stoichiometry of dissolution. As is shown later on, solution pH and temperature are key factors in determining both the thickness and composition of the leached layers. The thickness and composition, in turn, are shown to be related to the overall rate of dissolution, both during the initial and steady-state stages. In addition, it is shown that the open structure and the associated transport properties of the leached layers play an important role in determining the rate of dissolution. These pieces of evidence form the basis for demonstrating the applicability of the leached layer-surface reaction model to the dissolution of feldspars at elevated temperatures and pressures.

EXPERIMENTAL METHODS AND CALCULATIONS

The experimental methods in this study were the same as those described in Part I; therefore, only a brief synopsis is given here. All of the cleaved (≈1 cm × 1 cm) albite samples used in the experiments came from the same parent sample (locality: Amelia Court House pegmatite, VA, USA; obtained through Wards Scientific, Inc.). The endmember composition of this very pure albite was confirmed by electron microprobe analyses; the component oxides are listed in Table 1, Part I. Surface areas were measured with a multipoint BET gas adsorption technique, using Kr as the adsorbate gas. The adopted initial surface area used for all samples was 0.013 m^2 g^{-1}; the accuracy is estimated to be 20–30%. Geometric surface areas were more than an order of magnitude less, on the order of ≈0.0006–0.001 m^2 g^{-1}. Due to the fact that the initial surface area measurements were close to the limit of the BET technique, surface areas were not measured at the end of the experiments.

The dissolution experiments were carried out using a one-pass, tubular flow system constructed almost entirely of titanium; a schematic diagram of the system is shown in Fig. 1, Part I. Solutions were pumped by a HPLC pump through a preheating vessel before contacting the sample in a horizontally-positioned tubular autoclave vessel. The system pressure was maintained continuously at 170 bar by a back-pressure regulator.

Each experiment was started by pumping the inlet solution into the reactor which was at the desired temperature. Initially, the solution vaporized, until the pressure of the vapor exceeded the vapor saturation pressure. Once this occurred, the solution (entirely a liquid phase) flowed through the system and was sampled at the exit of the back pressure regulator. The start of any given experiment ($t = 0$) was a function of when the first drops of solution exited the regulator. It should be noted that this particular experimental operating procedure may induce a slight time lag with respect to the start of circulation, resulting from the time required to pass from a two phase, liquid-gas regime to a single, liquid phase regime. This phenomenon may have had a potential influence on the recorded release rate results for different operating temperatures close to $t = 0$, as will be discussed later on.

Flow rates ranged from 0.1–3.0 mL/min.; the calculated effective fluid-sample contact times were on the order of 0.1–3.0 min. Run times averaged 24 h, in some cases significantly longer experiments were run. At higher temperatures, run times were often less than 24 h (see Table 3, Part I for details). Due to the extremely short contact times between sample and fluid, the difference between the input and the output pH was not greater than 0.2 pH units at steady state. The pH of the inlet solutions was adjusted with HCl and KOH. In order to avoid competing ion effects that could have influenced the measured rates, no constant-pH or ionic strength buffers were added to the solutions. Solutions were left open to the atmosphere to equilibrate with CO_2. In-situ pH values were calculated using the EQ3/EQ6 code (Wolery, 1992; Wolery and Daveler, 1992); the in-situ pH values of the solutions are given in Table 2, Part I.

The output solutions were analyzed using standard atomic absorption (AA), atomic emission (ICP), and colorimetric techniques (see Part I for details). In general terms, the accuracy and precision of the Si data were superior to those of the Na and Al data. This especially held true for the measured concentrations of Na and Al from the 100°C experiments, where the concentrations of the measured elements were often less than 100 ppb. Uncertainties for Na and Al concentrations in the 0–100 ppb range were probably no better than ±10–20 ppb; this should be kept in mind when interpreting the results at 100°C. At concentrations ranging from 100–500 ppb, Na and Al analytical accuracy and precision were estimated to be 15–20%, and above 500 ppb, on the order of 10%. The precision and accuracy of the Si measurements, over the entire concentration range, were estimated to be 5–10%.

The release rates of Na, Al, and Si were calculated using the following formula (the applicability of this formula is discussed in the Appendix of Part I):

$$r = \frac{(C_{out})(\vartheta_0)(10^{-6})}{M\delta A}, \qquad (1)$$

where r is the stoichiometrically normalized release rate in mol m^{-2} s^{-1}, C_{out} is the output concentration of a given element in mg/L, ϑ_0 is the input flow rate in mL s^{-1}, M is the atomic weight (g mol^{-1}) of the element chosen, δ is the formula stoichiometric coefficient for the element chosen ($\delta \approx 1.0$ for Na and Al, and $\delta = 3.0$ for Si), and A is the total surface area in m^2. The stoichiometric coefficient serves to normalize the release rate, such that the calculated rate represents the overall dissolution rate of the mineral. Since the release rates were normalized to the stoichiometry of the solid, the case of congruent dissolution implies that the elemental release rates are all equal. At any given sampling interval, the total surface area used in the rate equation above was calculated from the initial surface area (i.e., A = mass × 0.013 m^2 g^{-1}). Since only the initial and final masses for each sample were known, the decrease in sample mass was calculated as a linear function of time. Unfortunately, due to the low surface areas, it was not possible to measure the effect of etch pit formation, etc., on the specific surface area (m^2 g^{-1}) as a function of time. The uncertainties in the non-steady-state release rates are difficult to estimate, since sample heterogeneities have a significant effect on the results (to be discussed further on). On the other hand, steady-state rates are less susceptible to this and therefore the uncertainties were estimated to be in the range of 0.2–0.3 log rate units (for more details, see Table 4 in Part I).

The chemical affinities of low albite and several other solid phases were calculated using the EQ3/EQ6 code (chemical affinity defined in Eqn. 6, Part I). The affinity calculations, based on the measured aqueous concentrations of Na, Al, and Si in the output solution, were made for conditions representing both the beginning and the end of each experiment. The chemical affinities, which have been shown alongside the release rates in Figs. 1–5, were used as a tool to predict which phases were thermodynamically favored to form secondary surface precipitates. The calculated saturation indices were based on a newly revised version of EQ3/EQ6 using the SUPCRT 92 (Johnson et al., 1992) thermodynamic database. Recent modifications to the SUPCRT 92 database were incorporated; these included the use of new thermodynamic data for Al-OH species and phases from Pokrovskii and Helgeson (1995). For this reason, the calculated chemical affinities for low albite differ by several kJ mol^{-1} from those reported in Part I. The uncertainties in the calculated affinities are estimated to be on the order of 1–3 kJ/mol. This estimate is based on data representing the end of experiment M (Fig. 1c). For each given phase, the uncertainty in the affinity was calculated by changing the measured elemental concentrations by the maximum estimated uncertainties in each element (M: ±5% in Si, ±10% in Na, ±50% in Al).

In order to directly verify the chemical affinity results, the presence or absence of surface precipitates was verified using SEM observations of the reacted surfaces for the samples whose release rates are shown in Figs. 1–5. As will be discussed in the Interpretations section, there were often quite large discrepancies between the chemical affinity predictions and the actual presence of secondary surface precipitates.

RESULTS

The experimental results are presented in terms of the time evolution of the release rates of Si, Al, and Na for dissolution experiments that were carried out with initial pH values (measured at 25°) of 2.0, 4.0, 5.7, 10.0, and 12.0; they are shown in Figs. 1, 2, 3, 4, and 5,† respectively. Each figure is composed of three subfigures showing the effect of increasing temperature (100, 200, and 300°C) on the release rates. The timescale representing the first few hours of dissolution was expanded in each figure in order to show more clearly the initial trends of the release rates. In all cases, the log rates are expressed in units of mol m^{-2} s^{-1}. The results below are discussed in terms of rates, although all figures show log rates. The pH values are given in terms of the initial value measured at 25°C, and in parentheses, the calculated value at temperature (indicated only if different from the 25°C value).

In general, for each set of pH and temperature conditions, more than one experiment was run (see Table 3, Part I); however, only one representative experiment was chosen for each figure. The results from experiments that have not been shown are discussed in those cases where there was some noteworthy phenomenon that was different from the release rate behavior shown. The results from all experiments are shown in Table 1.

Before specific results are discussed as a function of pH and temperature, it is useful to very briefly summarize some of the results common to the dissolution runs. The majority of the dissolution experiments can be characterized by elemental release curves showing a 'spike' followed by a monotonic decrease during the initial stages of dissolution. As can be seen in Figs. 1–5, the subsequent asymptotic approach to steady-state conditions depends on pH and temperature, both in terms of how large the monotonic decrease is and the time needed to attain steady state. At 300°C, however, the Si rate curves commonly did not show an initial spike, but rather a monotonic increase before a leveling-off at steady state occurred. A feature common to all dissolution runs at 100°C is a high degree of scatter in the Na release rates. It is noteworthy that the scatter is probably real and not due to analytical inaccuracy.

In comparing the trends of the elemental release curves at any given pH and temperature, it is important to note that the use of a log scale on the ordinate axis tends to magnify small differences between the various elemental release rates at low temperatures (100°C), where the overall rates of dissolution are very low. Inversely, at high temperatures (300°C) where dissolution rates are very high, small differences in the elemental release rates may appear to be insignificant on the diagrams, and yet are quantitatively important. The practical meaning of the above is that differences in rate curves cannot be directly compared based on log rates. An example of this can be seen in Fig. 1: a difference of 0.5 log rate units in the steady-state rate curves at 100°C is quantitatively (i.e., analytically) insignificant; inversely, a difference of 0.1 log rate unit in the initial rate curves at 300°C translates to a quantitatively important difference in rates.

Acid pH

pH 2.0

Figure 1a shows the evolution of the Si, Al, and Na release rates (sample A) over a time period of approximately 42 h at 100°C. Sodium and Al are preferentially released with respect to Si. All of the elemental release rates show a monotonic

† In Figs. 1–5, each elemental release rate is normalized with respect to the stoichiometry of albite. Note that the timescales representing the first few hours of dissolution have been expanded. The initial noncoincidence of the rate curves indicates non-stoichiometric dissolution (i.e., preferential release with respect to Si); the eventual convergence of the rate curves denotes congruent dissolution. In each figure, the chemical affinities of several phases have been indicated, based on the measured Na, Al, and Si concentrations at the beginning and the end of the experiments (as denoted by the arrows). Positive affinities denote undersaturation; negative affinities denote supersaturation (indicated by *). The estimated uncertainties in the affinities are 1–3 kJ/mol. Mineral phase abbreviations are as follows: alb = low albite, analc = analcime, boeh = boehmite, corund = corundum, diasp = diaspore, gibbs = gibbsite, kaol = kaolinite, natro = natrolite, qtz = quartz.

Table 1. Elemental release relationships and calculated depths* of preferential leaching.

Sample	pH (25°C)	pH (T)	Temp (°C)	Run time (hours)	Preferential release relationships with respect to Si; leaching depths in Å (time in hours)		Comments
					Na : Si	Al : Si	
YB	0.7	1.3	300	19.42	Na ≈ Si	Al > Si → Al ≈ Si	1
A	2.0	2.0	100	42.15	Na > Si; 1379 (1.5) a*	Al > Si; 61 (1.5)	no precip. (SEM); Na ↓
B	2.0	2.0	200	47.80	Na > Si; 1533 (0.35)	Al ≈ Si → Si > Al; -7 (0.35)	Al precip. (SEM) (sparse)
C	2.0	2.0	200	86.30	Si > Na; -504 (0.60) (?)	Si > Al; -996 (0.60) (?)	incomplete initial Na data, 3
L	2.0	2.0	200	23.70	Na > Si; 481 (0.17)	Al > Si; 68 (0.17) → Si > Al	
D	2.0	2.2	300	24.05	Na > Si	Al ≈ Si	1, no sample recovered, 3
E'	2.0	2.2	300	0.08	Na > Si	Al > Si → Si > Al	1, 3
E"	2.0	2.2	300	2.27	Na > Si	Si > Al	1, 3
G	2.0	2.2	300	0.67	Na > Si; 1405 (0.20)	Si > Al	3
M	2.0	2.2	300	24.83	Na > Si; 151 (0.10)	Si > Al	Al precip. (SEM)
RD	3.4	3.4	300	24.25	Na ≈ Si	Si > Al	1, 3
VB	4.0	4.0	100	24.20	Na > Si; 158 (0.40)	Al > Si → Si > Al → Al ≈ Si b*	no precip. (SEM)
VA	4.0	4.0	200	23.42	Na > Si; 25 (0.10)	Al > Si → Si > Al	Al precip. (SEM)
VE	4.0	4.0	300	23.15	Na > Si; 245 (0.37)	Al ≈ Si → Si > Al	Al precip. (SEM)
Q	5.7	5.7	100	44.17	Na > Si; 166 (0.97)	Al > Si; 6 (0.97)	no precip. (SEM); Na & Al ↓
P	5.7	5.6	200	24.37	Na > Si; 148 (1.25)	Al > Si → Si > Al c*	Al precip. (SEM)
N	5.7	5.7	300	24.08	Na > Si; 249 (0.18)	Si > Al	Al precip. (SEM)
RC	5.7	5.7	300	24.00	Na > Si	Si > Al	1, 3
YA	5.7	5.7	300	248.0	Na ≈ Si	Si > Al	1, 3
YH	6.8	6.8	300	4.33	Na > Si	Al> Si → Si > Al	1
YF	8.7	7.6	300	5.42	Na > Si	Al ≈ Si	1
YG	9.6	7.7	300	10.25	Na > Si	Al ≈ Si	1
TE	10.0	8.4	100	24.58	Na > Si; 800 (0.67)	Al > Si; 251 (0.67)	no precip. (SEM); Na & Al ↓
TA	10.0	7.6	200	24.00	Na > Si; 1227 (0.43)	Al ≈ Si; 8 (0.43)	no precip. (SEM); Na ↓
TD	10.0	7.7	300	21.03	Na > Si; 94 (0.20)	Si > Al; -65 (0.2)	no precip. (SEM); Na ↓
RE	11.0	8.6	300	24.00	Na > Si	Al ≈ Si	1,4
YE	11.0	8.6	300	6.08	Na > Si	Al ≈ Si	1,4
SA	12.0	10.3	100	23.95	Na > Si; 63 (5.12)	Al > Si → Si > Al; -67 (5.12)	4, no precip. (SEM); Na ↓ , Al ↑
SF	12.0	9.3	200	24.00	Na > Si; 439 (0.43)	Al > Si; 126 (0.43)	4, no precip. (SEM); Na ↓
SB	12.0	9.2	300	23.87	Na ≈ Si	Al > Si	2, 4 precip. (SEM); Na ↓
YD	12.0	9.2	300	13.09	Na > Si	Al > Si	1, 4
YC	13.1	10.0	300	7.17	Na > Si	Al > Si	1, 4

* Depths based on a linear depletion gradient (see text for details); negative depths indicate preferential leaching of Si
a* Interpretation: preferential release of Na over Si, depth of leaching = 1379 Å (depth based on time when release curves became coincident)
b* Interpretation: The Al rate data suggest the preferential release of Al over Si, followed by the precipitation of an Al phase, which then was redissolved, resulting in an increasing and then constant Al release rate which was equal to the Si rate
c* Interpretation: initial preferential release of Al over Si, followed by preferential release of Si over Al, due to precipitation of an Al-phase
1 insufficient data for determination of leaching depths
2 SEM/EDS results suggest that the precipitate is not boehmite; the pronounced Ca and Si peaks perhaps indicates a zeolite phase
3 precipitation of an Al-phase likely, but *not* substantiated by SEM observations
↓ ↑ Na and/or Al: Depth of leaching based on modified (decreased ↓ or increased ↑) rate curve, such that the adjusted rate curve at *steady state conditions* equals the Si rate curve
4 Na depths (release) significantly decreased due to Na impurity in KOH input solution- see text

decrease over the first 2 h of dissolution. The chemical affinities at the beginning and the end of the 100°C run (denoted by arrows in Fig. 1) did not predict the supersaturation of the solution with respect to any Al-bearing phases. The lack of precipitates was verified by SEM (see Fig. 6a).

The initial behavior of the release curves at 200°C (Fig. 1b) was similar to that at 100°C, except that the degree of scatter in the Na rates was considerably less. The calculated chemical affinities suggested that diaspore, and perhaps boehmite as well, potentially could have precipitated at the

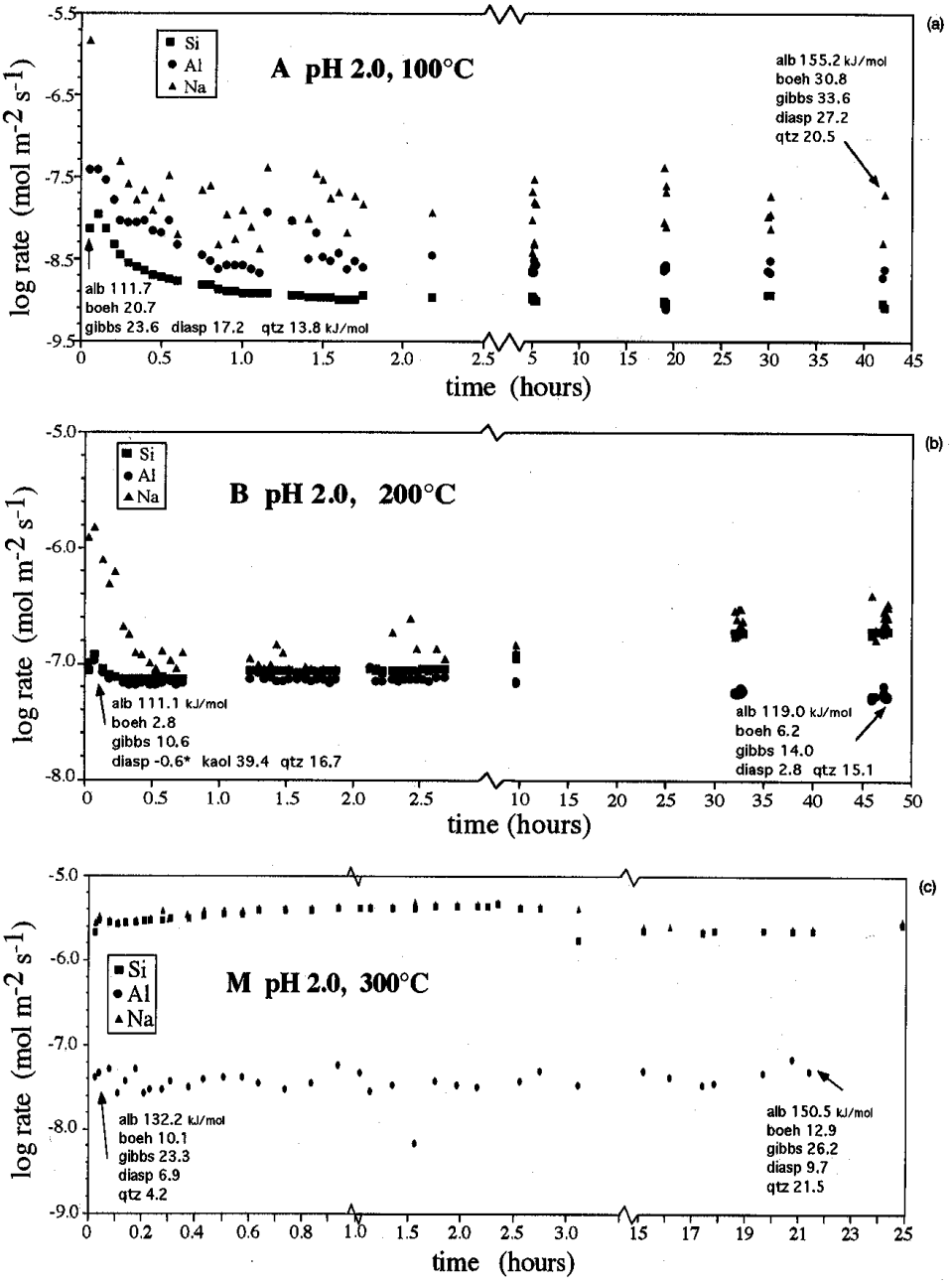

FIG. 1. The time evolution of the Si, Al, and Na (log) release rates at pH 2.0. Note the initial preferential release of Na and Al vs. Si at 100° (a) and 200°C (b). The sharp drop in the Al rate curve at 300°C (c) reveals the precipitation of a secondary Al phase (boehmite ?) on the surface over the course of the experiment.

beginning of the experiment. After 48 h of dissolution, the solution was predicted to be slightly undersaturated with respect to both diaspore and boehmite. The divergence of the Si and Al rate curves with time ($t > 10$ h) may be due to the localized precipitation of an Al phase. SEM images revealed that the surface was very corroded and had a high concentration of etch pits. Precipitates possibly occurred in a few of the etch pits (see bottom edge of Fig. 6b).

At 300°C (pH 2.2) the rate curves for all three elements were different with respect to the previous results, as can be seen in Fig. 1c (sample M). The Na and Si release rates did not display a prominent initial spike and subsequent monotonic decrease. Even though the Si and Na rates were almost identical over the entire run, there is evidence for the preferential release of Na at the very outset of the experiment. This type of behavior may be real, and its importance is discussed further on.

The positive chemical affinities of various Al phases determined at the beginning and end of the experimental run were not indicative of solution supersaturation. Nonetheless, SEM observations confirmed that dense masses of bladed crystals had precipitated on the surface (see Fig. 6c). SEM/EDS analyses of the precipitated crystals revealed the presence of only Al and O. The exact identity of the precipitates could not be confirmed directly by X-ray diffraction due to the small quantities present. Nonetheless, the acicular Al precipitates are thought to be boehmite, due to their close morphological resemblance to those precipitated on albite and identified by X-ray diffraction in Hellmann et al. (1989). The surface coverage of the crystals was uniform in some areas, whereas other areas were barren of crystals.

pH 4.0

The results at 100°C (sample VB; Fig. 2a) revealed some of the same trends (and scatter) as were shown at pH 2.0. Sodium was preferentially released with respect to Si. The Al rate curve showed that Al was preferentially released with respect to Si at $t = 2$ min. The trough in the Al rate curve is most likely due to the transient precipitation of an Al phase. Note that at $t \geq 0.2$ h, the Al rate rose sharply and then attained steady state. The calculated chemical affinities showed that three Al phases, diaspore (−9.2 kJ/mol), gibbsite (−2.7 kJ/mol), and boehmite (−5.6 kJ/mol), were predicted to precipitate at the beginning of the experiment. Only the chemical affinity of diaspore (−0.16 kJ/mol) was negative at the end of the experiment; both gibbsite (6.3 kJ/mol) and boehmite (3.4 kJ/mol) had positive chemical affinities. SEM images did not reveal the presence of surface precipitates (note: images were taken of rehydrolyzed sample VB′). This may have been due to the precipitates having formed in small cracks or etch pits that were not amenable to direct SEM imaging. The more likely reason is that any initially formed precipitates were redissolved during the course of the experiment.

At 200°C (Fig. 2b, sample VA) Na and Al were preferentially released during the initial period of dissolution. The initial high Al release rate led to the solution becoming supersaturated with respect to boehmite (−2.1 kJ/mol) and diaspore (−5.5 kJ/mol). This supersaturation led to the precipitation of an Al phase, as revealed by SEM. Based on the fact that the Al rate continuously diverged from the Si rate over time may imply that precipitation occurred during the course of the experiment, despite the fact that the chemical affinities of boehmite and diaspore at the end of the experiment predicted undersaturation of the solution with respect to these two phases.

Dissolution at 300°C (sample VE) is shown in Fig. 2c. Sodium was preferentially released with respect to Si at the outset of dissolution, thereafter their rates were nearly identical. The behavior of the Al rate curve implied that an Al phase precipitated during the initial stages of dissolution (negative chemical affinities for boehmite and diaspore), and continued to precipitate over the course of the experiment. SEM images of the surface showed the sparse presence of bladed precipitates on the extremely etched and pitted surface.

Neutral pH

The neutral pH region mainly encompassed dissolution experiments using deionized water with a pH of 5.7 at 25°C. In addition, the results from two other experiments with starting pH values at 25°C of 6.8 and 8.7 have also been included in the neutral pH grouping, due to the fact that their dissolution behavior (see Part I) showed no pH dependence, and was therefore similar to the behavior recorded for the experiments run at pH 5.7.

pH 5.7

The results at 100°C and pH 5.7 are shown in Fig. 3a (sample Q). Both Na and Al were preferentially released at the beginning of dissolution. It is not certain whether the discontinuity and divergence in the release rate trends at $t > 22$ h can be attributed to the failure of the HPLC pump and subsequent resumption of circulation (which occurred over $t = 22.6$–24.7 h). Based on the calculated chemical affinities, the solution was supersaturated with respect to diaspore at the end of the experiment. No precipitates were observed by SEM (sample Q′).

Figure 3b shows the results for dissolution at pH 5.7 and 200°C (sample P). Sodium was preferentially released over Si at the onset of dissolution. The Al rate initially exceeded the Si rate at the very start ($t \leq 3$ min) of the experiment. The behavior of the Al rate curve is indicative of the precipitation of an Al phase over the course of the experiment, as confirmed by SEM. Despite direct evidence for precipitation, the chemical affinity results show that the solution was undersaturated with respect to such phases as boehmite and diaspore.

SEM images of the sample surface after dissolution (Fig. 6d, e) show the heterogeneous nature of dissolution. Note how the negative faces of the two large depressions (etch pits?) in Fig. 6d have a much higher density of precipitated crystals than the surrounding surfaces, which are relatively barren of precipitated crystals and show only small etch pits. This indicates that the localized level of solution supersaturation within the two large pits was much higher than in the bulk solution in contact with the adjacent flat crystal surfaces. The prismatic precipitates formed at 200°C may be either diaspore or boehmite, based on their morphologies. Attempts at

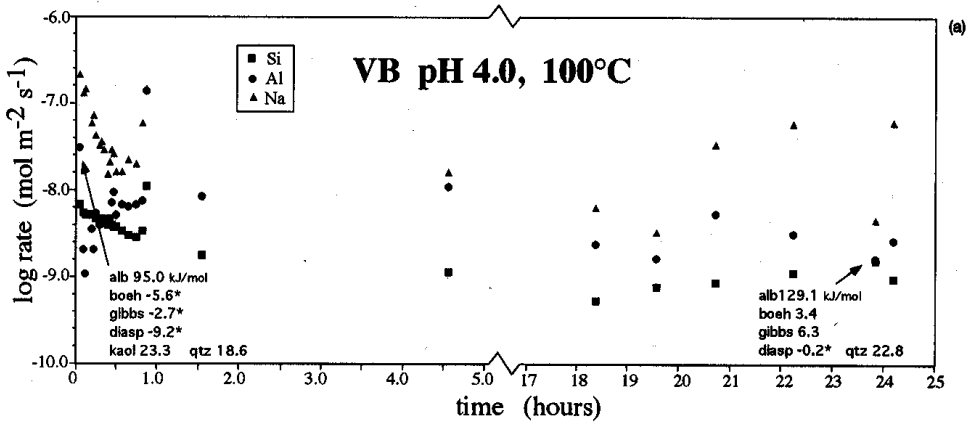
(a)
VB pH 4.0, 100°C
Si
Al
Na
log rate (mol m-2 s-1)
time (hours)
alb 95.0 kJ/mol
boeh -5.6*
gibbs -2.7*
diasp -9.2*
kaol 23.3 qtz 18.6
alb129.1 kJ/mol
boeh 3.4
gibbs 6.3
diasp -0.2* qtz 22.8

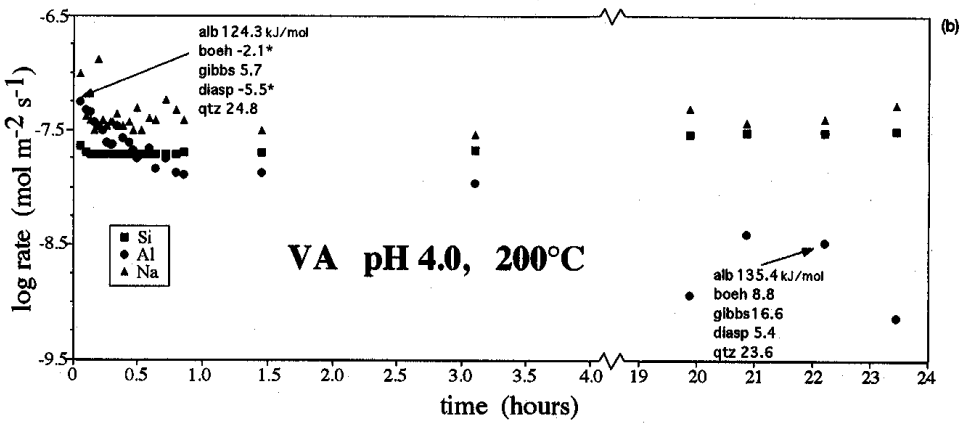
(b)
VA pH 4.0, 200°C
Si
Al
Na
log rate (mol m-2 s-1)
time (hours)
alb 124.3 kJ/mol
boeh -2.1*
gibbs 5.7
diasp -5.5*
qtz 24.8
alb 135.4 kJ/mol
boeh 8.8
gibbs16.6
diasp 5.4
qtz 23.6

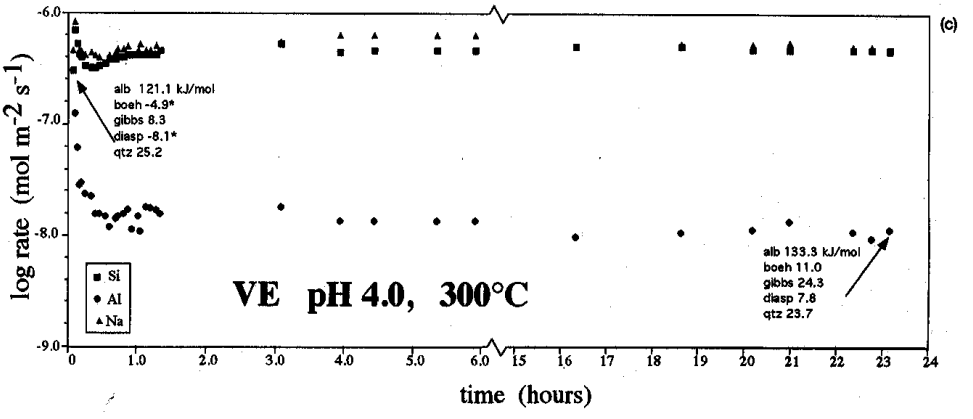
(c)
VE pH 4.0, 300°C
Si
Al
Na
log rate (mol m-2 s-1)
time (hours)
alb 121.1 kJ/mol
boeh -4.9*
gibbs 8.3
diasp -8.1*
qtz 25.2
alb 133.3 kJ/mol
boeh 11.0
gibbs 24.3
diasp 7.8
qtz 23.7

X-ray diffraction analysis were unsuccessful, due to the small quantities of crystals present.

Figure 3c (sample N) shows the results of dissolution at 300°C and pH 5.7. Sodium is preferentially released over Si. As opposed to the results at pH 2.0 and 4.0 (300°C), the initial Na and Si rate curves display prominent spikes, followed by monotonic decreases to steady-state values. The Al rate curve is suggestive of the rapid initial precipitation of an Al phase. It cannot be ascertained, however, whether the initial rate of Al release exceeded that of Si. This is an example of how a precipitation process can obscure the signal of the intrinsic hydrolysis processes occurring at the surface and within the leached structure. Note that over an extended period of time, the Al rate curve asymptotically approaches the Si rate curve. The calculated chemical affinities at the beginning and end of the experiment indicate that the solution was undersaturated with respect to potential Al precipitating phases. SEM images show that the hydrolyzed surface is very corroded and generally barren of secondary precipitates. However, careful observation within cracks and crevasses revealed the sparse occurrence of bladed aggregates of crystals.

pH 6.8, 8.7

Two samples were hydrolyzed at 300°C under mildly alkaline conditions. In both experiments, the rates were only measured at the beginning and at the end of the runs. Dissolution of sample (YH) showed the initial preferential release of Al and Na with respect to Si. The other sample (YF) was hydrolyzed at pH 8.7 (7.7). Under these conditions only Na was preferentially released with respect to Si, whereas Al was congruently released with respect to Si. Both experiments revealed that Na, Al, and Si were congruently released at the end of the experiments.

Basic pH

Note: The reagent grade KOH used to adjust the pH of the stock solutions was contaminated by Na. The Na rates shown in Figs. 4 and 5 are blank-corrected. This was done by adjusting the Na release curves downward, such that at steady-state conditions, the Na and Si curves were identical (note: the same method of release rate adjustment was described earlier in detail). The effect of Na in solution is to decrease the preferential release of Na from the structure (Petit et al., 1990). This effect should be most pronounced at pH 12.0.

pH 10.0

Figure 4a (sample TE) shows the results for dissolution at 100°C and pH 10.0 (8.5). Sodium and Al showed preferential leaching with respect to Si in the beginning stages of dissolution. Over the period of $t > 2$ h, there was a marked divergence of the Na rate curve from the Si and Al curves. This type of divergence was not noted upon redissolution of the sample. Even though the formation of a secondary Al-Si precipitate cannot be ruled out, the divergence is more likely to be due to analytical uncertainty in Na. Diaspore is the only solid that had an affinity close to zero. No solid phases were observed by SEM (sample TE′).

The dissolution results at 200°C and pH 10.0 (7.6) are shown in Fig. 4b (sample TA). The initial stages of dissolution were characterized by the preferential release of Na. As was the case at 100°C, the first measured rate ($t \leq 1.8$ min) revealed the preferential release of Al over Si. Subsequently, the Al and Si rates became roughly equal ($t \geq 0.5$ h). According to the chemical affinity calculations, the solutions at both the beginning and the end of the experimental run were at or above saturation with respect to any of the solid phases accounted for by the calculations. SEM images did not reveal any surface precipitates.

At 300°C and pH 10.0 (7.7), the behavior of the Si rate curve (Fig. 4c, sample TD) differed from the preceding runs at lower temperatures since it displayed a monotonic increase and then a leveling-off at steady state. The degree of Na preferential release was minimal, except at the very onset of dissolution; thereafter, the Na rates were roughly equal to the Al and Si rates. Except for the initial data point showing the preferential release of Si over Al, both rates were equal over the course of the experiment. No solid phases were predicted to have precipitated, and SEM did not reveal the presence of any precipitates.

In addition to the experiments at pH 10.0, one sample (YG) was hydrolyzed at pH 9.6 (7.7) and 300°C. This run was only sampled at the beginning and the end of the experiment. Al and Si were congruently released, and only a slight initial preferential release of Na with respect to Si was observed.

pH 11.0, 12.0

At pH 11.0 (8.6) two experiments were run, both at 300°C. In both cases, the rates of Si and Al release at the beginning and at the end of the experiments were equal. A small degree of Na preferential leaching occurred.

The results at pH 12.0 (10.3) and 100°C are shown in Fig. 5a (sample SA). Sodium was preferentially released with respect to Si. The first Al rate measurement indicated the preferential release of Al over Si; thereafter, the Al rate curve always remained below the Si curve. While the overall preferential release of Si over Al is probably real (for $t < 2$ h), it is possible that the steady-state Si and Al release rates were equal and that the offset in the curves is due to analytical uncertainty (i.e., [Al] measurements that were too low by 20 ppb with respect to [Si]). It is interesting to note that when this sample was rehydrolyzed (SA′), it was found that Al was preferentially released with respect to Si. This finding suggests that under these pH and temperature conditions, the preferential release of either Al or Si is probably not signifi-

FIG. 2. The time evolution of the Si, Al, and Na (log) release rates at pH 4.0. The behavior of the 100 (a) and 200°C (b) rate curves shows many of the same characteristics that were observed at pH 2.0, such as the preferential release of Na and Al vs. Si. The divergence of the Al rate curves at 200 (b) and 300°C (c) was due to the precipitation of an Al phase. Precipitation occurred even though the chemical affinities did not always predict that the bulk solution was supersaturated with respect to Al phases which potentially could have precipitated.

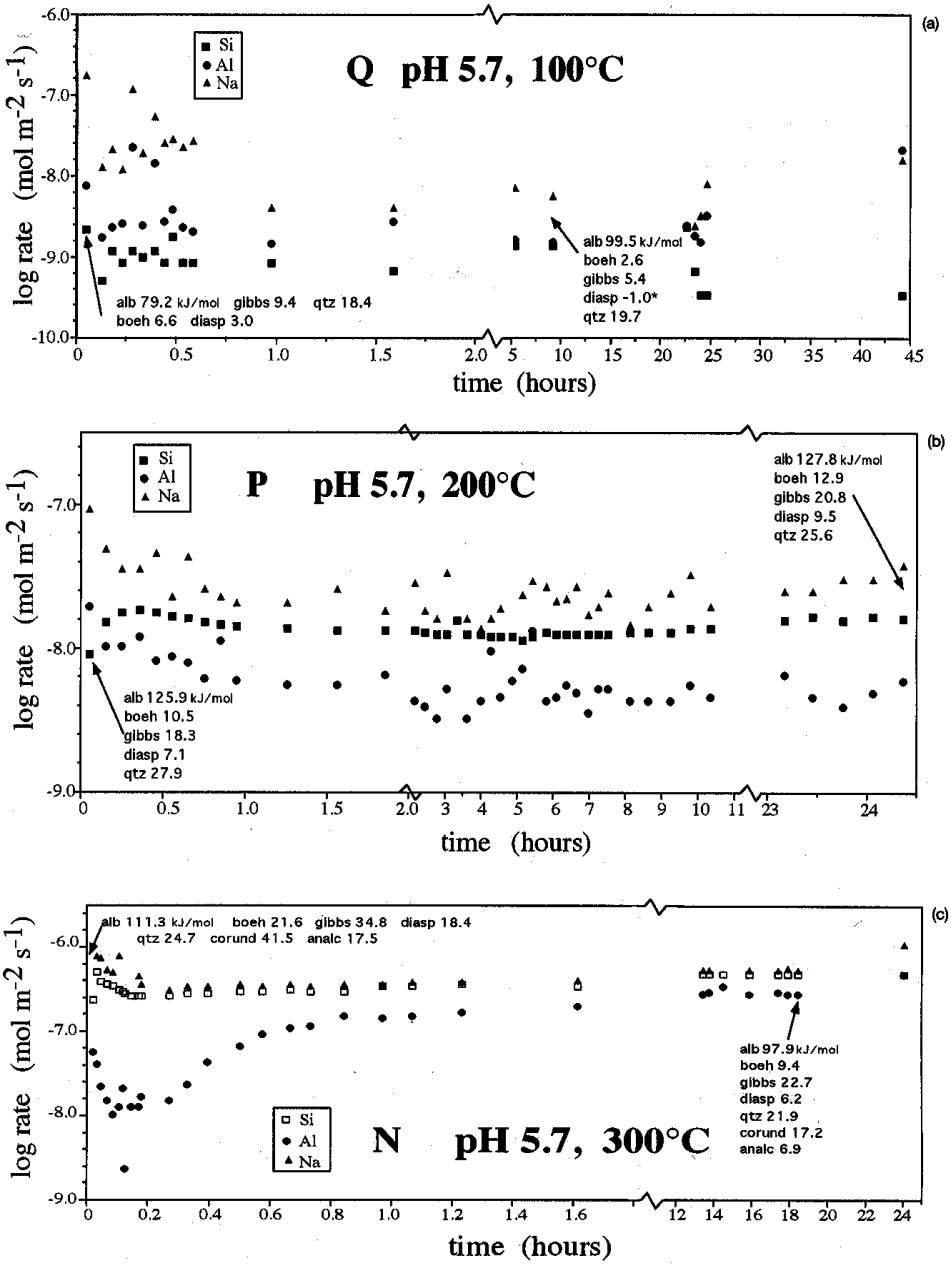
(a)
Q pH 5.7, 100°C
Si
Al
Na
log rate (mol m-2 s-1)
time (hours)
alb 79.2 kJ/mol gibbs 9.4 qtz 18.4
boeh 6.6 diasp 3.0
alb 99.5 kJ/mol
boeh 2.6
gibbs 5.4
diasp -1.0*
qtz 19.7
(b)
P pH 5.7, 200°C
alb 127.8 kJ/mol
boeh 12.9
gibbs 20.8
diasp 9.5
qtz 25.6
alb 125.9 kJ/mol
boeh 10.5
gibbs 18.3
diasp 7.1
qtz 27.9
(c)
alb 111.3 kJ/mol boeh 21.6 gibbs 34.8 diasp 18.4
qtz 24.7 corund 41.5 analc 17.5
N pH 5.7, 300°C
alb 97.9 kJ/mol
boeh 9.4
gibbs 22.7
diasp 6.2
qtz 21.9
corund 17.2
analc 6.9

cant and the noncongruency is simply due to analytical uncertainty. The chemical affinity results showed precipitation of secondary phases to be unfavorable. SEM showed no precipitates (sample SA′).

Figure 5b (sample SF) shows the dissolution results at 200°C and pH 12.0 (9.3). Sodium was preferentially released with respect to Si and Al during the initial stages of dissolution. The degree of Al preferential release over Si (for $t < 0.25$ h) was significant. No secondary phases were predicted or observed.

The results of dissolution at 300°C and pH 12.0 (9.3) are shown in Fig. 5c (sample SB). The Si rate curve displayed a monotonic increase and then a leveling-off at steady state, a trend similar to the Si rate curve at pH 10.0 (7.7) in Fig. 4c. Sodium was not preferentially released with respect to Si and Al (due most probably to the Na contamination problem). The preferential release of Al was extremely pronounced. It is not known why this particular sample displayed such an unusually elevated initial rate of Al release.

An SEM image (Fig. 6f) revealed the sparse presence of needle-like precipitates. Their needle-like structure and morphology were different from the acicular crystal aggregates observed in Fig. 6c. SEM/EDS analyses showed Si, Ca, O, Al, and Na to be the primary elements present (peak height ratios of 6:3:3:1:0.3, respectively). Based on their morphology and chemical composition, it is suggested that these crystals are possibly a zeolite phase. The chemical affinity results did not predict the precipitation of a solid phase. This may be a function of the incomplete representation of zeolite phases in the EQ3/EQ6 database.

Another sample (YD) was also run at 300°C. The lack of continuous sampling only allowed for the observation of the preferential release (on the order of 0.4 log rate units) of Al over Si at the onset of dissolution; after 13 h the rates were equal. The initial rate of Al release was almost 1.5 orders of magnitude less than it was for sample SB. Nonetheless, both of these results confirm that the degree of Al preferential release is significant at these pH and T conditions.

Under pH conditions still more severe than the conditions described above, another sample (YC) was hydrolyzed at 300°C and pH 13.1 (10.0). At the beginning of the experiment Al was preferentially released (a significant difference of 0.3 log rate units was measured). Dissolution was congruent after 7.2 hours of dissolution.

INTERPRETATION OF DATA

In a general manner, the dissolution of any mineral can be described in terms of the adsorption of reactant molecules at chemically reactive sites, the hydrolysis of bonds (a multistep process), and the detachment of product molecules and/or atoms. When one considers complex multicomponent oxides such as feldspars, dissolution is not only a function of reactions occurring at the solid/solution interface, but it is also dependent on reactions taking place at significant depths within the structure. The reactions that occur within the structure are elementally rate-specific; that is to say that each element within the structure may react at a different rate with the reactant molecules which diffuse into the structure. The differential rates of detachment lead to the formation of leached layers that have a chemical composition and a physical structure different from that of the bulk mineral. The outward diffusion of product species through the leached layers may be influenced by reactions with elements comprising the leached layer. The outward flux of products may also lead to the supersaturation of the solution at the solid/liquid interface, thereby leading to the precipitation of a secondary phase(s) on the surface.

It is specifically the time evolution of the release rates, from the initial stages to steady-state conditions, that offers the best means for understanding the complexity of the feldspar dissolution process. The discussion and interpretation of the elemental release rate curves is presented in the following manner: initial reactions at the surface, progression of a reaction front into the structure, monotonic decrease in the rates of release, attainment of steady-state rates and potential evolution of these rates, depths of preferential release, chemical speciation of leached layers, diffusion within leached layers, structural interdependence of Na, Al, and Si release rates, dissolution rates and leached layer depths, and precipitation of secondary Al phases on the surface.

Based on the processes listed above, a detailed interpretation is made of a set of rate curves obtained for a sample (expt. B) hydrolyzed at pH 2.0 and 200°C (Fig. 1b). This set of rate curves is fairly typical for those obtained under acid conditions, in the absence of major surface coverage by precipitates. This set of rate curves was specifically chosen since they could be compared (qualitatively) to results from a similar study (Hellmann et al., 1990), where albite was hydrolyzed at 225°C and pH 0.7. Specifically, use is made of data (Hellmann et al., 1990) representing the consumption of protons as a function of time. The consumption of protons was determined from the difference in the pH of the input and the output solution, both measured at 25°C. Although the experimental conditions were not exactly identical with those of the present study, the H^+ consumption trend offers important qualitative evidence for the interpretation of the rate curves discussed below. The rate curves obtained in the present study for different pH and temperature conditions are not explicitly treated, except in the case where they require a different interpretation than given for sample B.

Initial Surface Reactions: Acid pH

The initial elemental rate curves for Na, Al, and Si can be described in terms of an asymmetric pulse or spike resulting from

FIG. 3. The time evolution of the Si, Al, and Na (log) release rates at pH 5.7. Sodium was preferentially released at all temperatures (a–c). The sharp drop in the rates at 100°C (a) at $t = 22–25$ h was due to a pump failure. During the initial stages of dissolution, Al was also preferentially released, even though Al precipitation occurred at 200 (b) and 300°C (c). The Al rate curve at 300°C (c), which displayed a sharp drop followed by a gradual increase, is indicative of initial precipitation reactions followed sequentially by the redissolution of the precipitates and overall congruent dissolution.

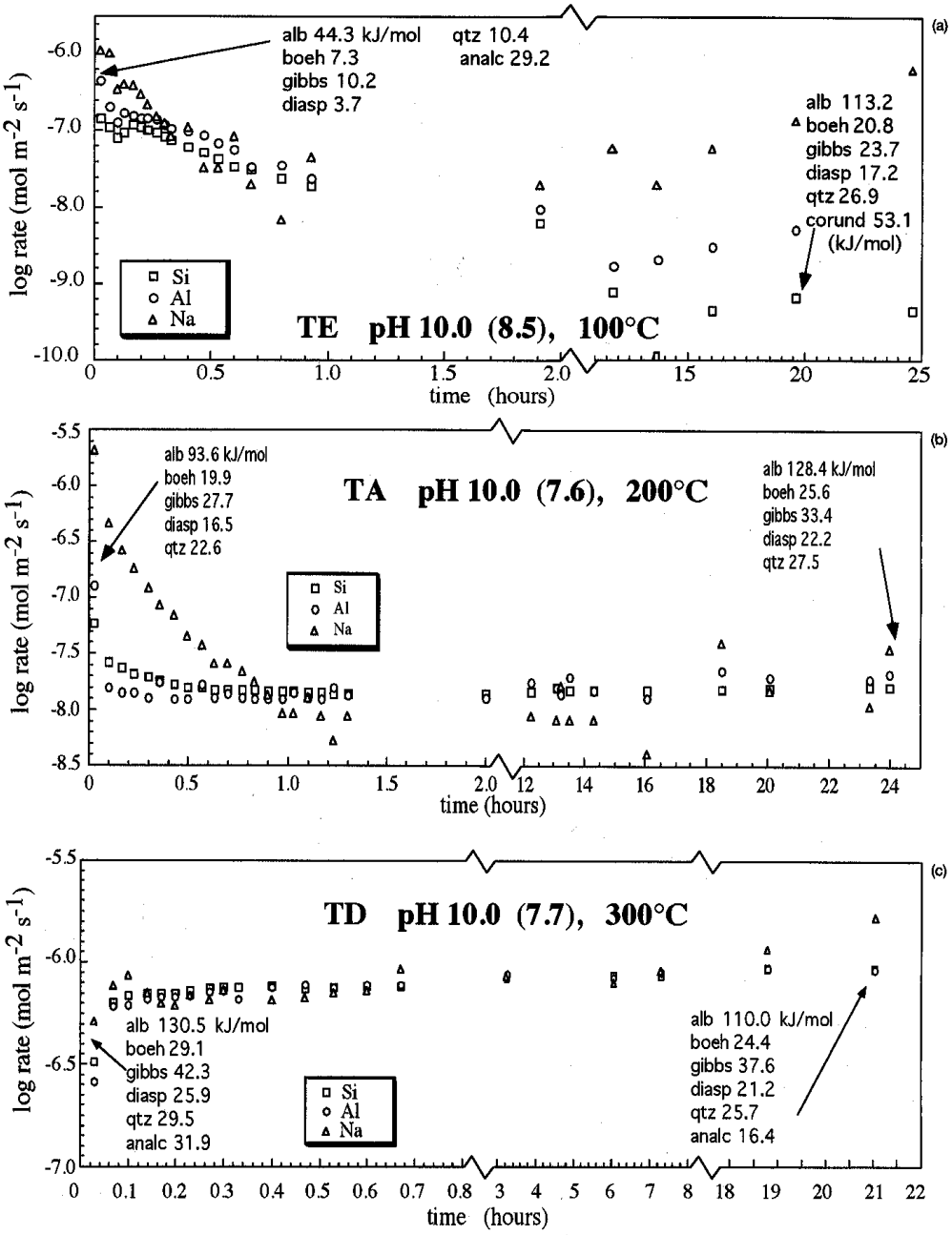

FIG. 4. The time evolution of the Si, Al, and Na (log) release rates at pH 10.0 (pH meas. at 25°C). Sodium was preferentially released at all temperatures. At 100°C (a), Al was preferentially released, but at 200 (b) and 300°C (c), Al and Si were congruently released (within the error of analyses).

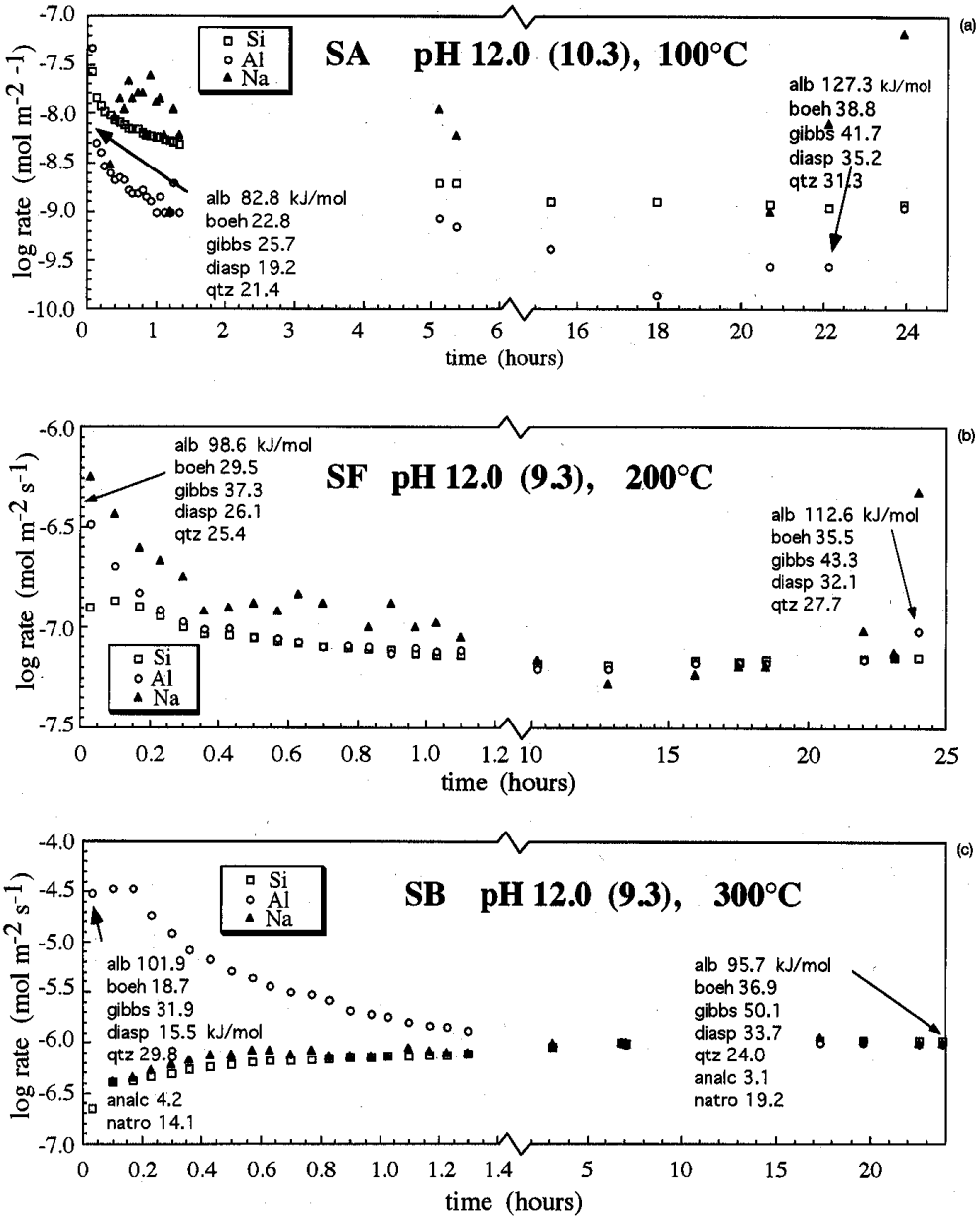

FIG. 5. The time evolution of the Si, Al, and Na (log) release rates at pH 12.0 (pH meas. at 25°C). Sodium was preferentially released, except at 300°C (c). As noted in the text, the degree of Na release was adversely affected by a Na impurity in the initial stock solution. Aluminum hydrolysis was either roughly congruent (100°C (a); note that nonconvergence is attributed to analytical uncertainty), or initially greater than Si at 200 (b) and 300°C (c).

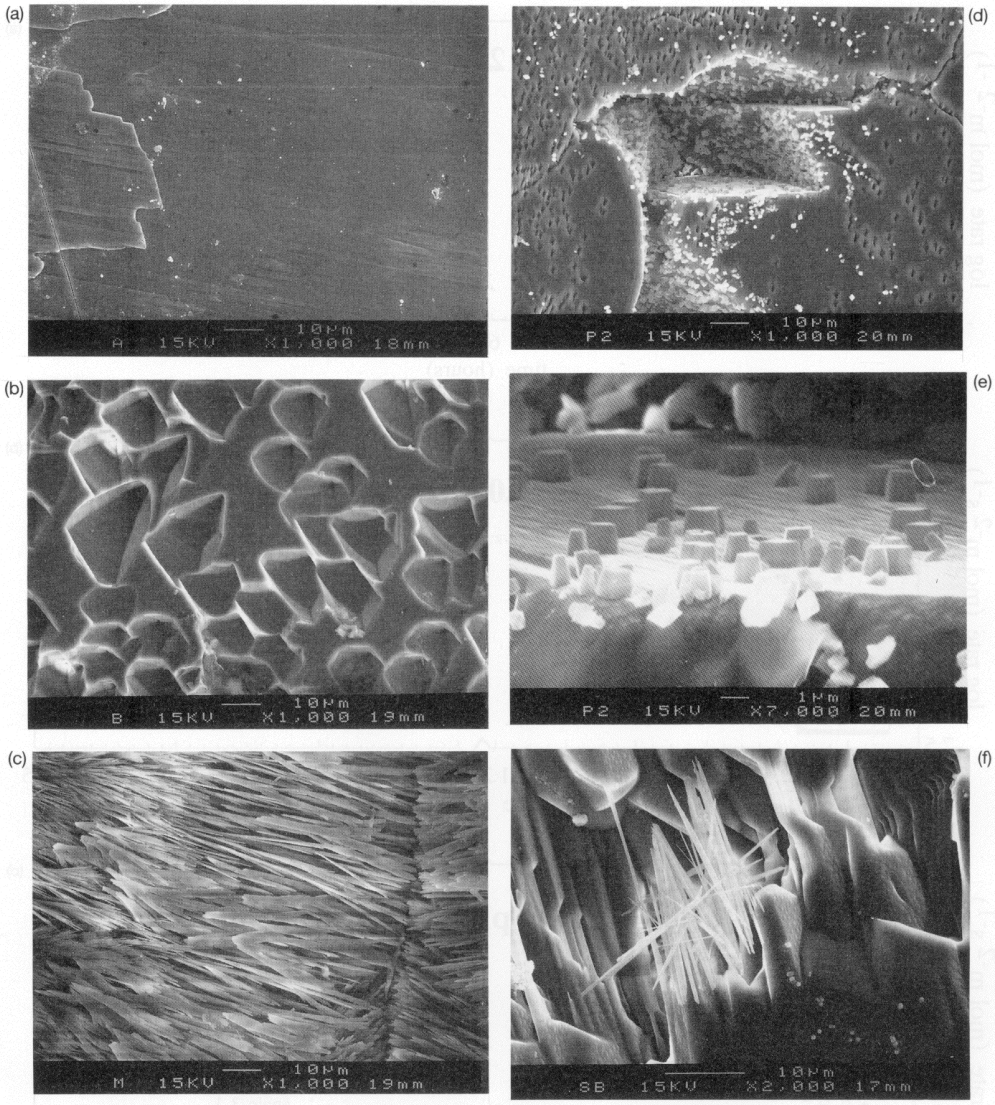

FIG. 6. (a) A (010) surface of albite after dissolution at pH 2.0 and 100°C. The surface shows few signs of chemical attack and is relatively devoid of surface fines. (b) A highly etched (010) surface after dissolution at pH 2.0 and 200°C (with possible precipitates occurring in some etch pits- see lower portion of image). (c) Dissolution at pH 2.0 and 300°C resulted in the massive precipitation of bladed boehmite (?) crystals. Note the high degree of interconnected porosity. (d) A (010) surface after dissolution at pH 5.7 and 300°C. Note the large depression (etch pit?) in the center, surrounded by a surface with numerous small etch pits. (e) The elevated degree of supersaturation of the solution within the large pit led to the localized precipitation of numerous prismatic crystals. (f) Precipitated zeolite (?) crystals on a sample subjected to dissolution at pH 12.0 (9.3) and 300°C.

a rapid increase in the release rate from zero to a maximum value, followed by a monotonic decrease to a plateau rate value (see Fig. 7, trends A → B → C). The extremely sharp increase in the release rates of Na, Al, and Si from $t = 0$ to their respective maximum rates can be attributed to rapid ion exchange and hydrolysis reactions that occur at the surface, where the surface is defined to extend one unit cell into the structure. The initial increase in rates (trend A, Fig. 7), which occurs over approximately 0.1 h, is mirrored by a similarly sharp increase in the consumption of protons (trend A, Fig. 8). This is the result of H^+ being consumed by ion exchange with Na^+ and adsorption of H^+ on surface silanol (Si-OH) and aluminol (Al-OH) groups. Adsorption of H^+ eventually leads to hydrolysis and detachment of Si and Al from surface sites.

The rapid kinetics of the initial stage of dissolution is due to several factors. First, the coordination environments and the chemical speciation of Na, Al, and Si at the surface differ from those deeper within the bulk structure, thereby making surface atoms far more reactive. In general, surface metal atoms (Al, Si) are coordinated to one or more OH groups; therefore, there are fewer metal-bridging oxygen bonds that require hydrolysis for complete detachment of the metal to occur. In addition to this, access of reactant molecules to reactive sites is not impeded by diffusion through a solid structure. The reactions which take place at surface sites occur in the presence of a free fluid, where diffusion rates are very rapid (diffusion coefficient D values range from 10^{-4}–10^{-5} $cm^2\ s^{-1}$). Therefore, the rates of detachment control the kinetics of hydrolysis at surface sites.

The enhanced reactivity of surface sites may also be caused by an elevated surface strain energy. The creation of a fresh surface by a cleavage process necessarily results in the rupture of bonds that may lead to a configuration of surface atoms having a perturbed coordination and/or chemical environment (see discussion by Petrovich, 1981a,b, for example). Evidence in accord with this is based on the results of surface titrations of albite powders before and after thermal annealing at 900°C. The degree of proton consumption of the thermally annealed powders was over an order of magnitude lower than

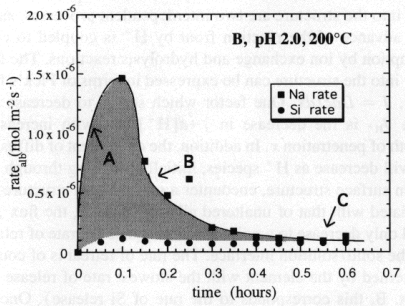

FIG. 7. Initial Na and Si rate curves (stoichiometrically normalized) at pH 2.0 and 200°C. These rate curves show behavior typically observed at most temperature and pH conditions: a very rapid initial increase (A), a monotonic decrease (B), an attainment of an initial steady state (C). Leached layer thicknesses were calculated directly from the excess moles of Na (or Al) released with respect to Si, as represented by the shaded area.

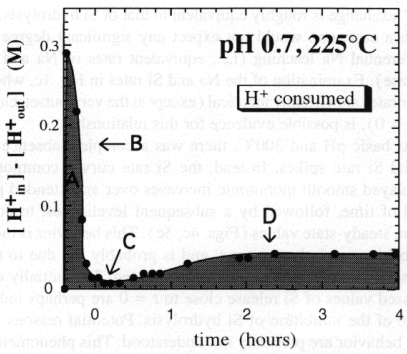

FIG. 8. The time evolution of the number of protons consumed during dissolution at pH 0.7 and 225°C. Note the similarity in the trend A → B → C with that shown in Fig. 7. Data to the left of $t = 0$ were obtained as the reactor was being heated. Data from Hellmann et al., 1990.

the untreated powders. This suggests that an annealed surface (which has a more stable configuration of surface atoms) is chemically less reactive (R. Hellmann, unpubl. data; see also results in Schott, 1990).

Of course, another reason for the initial dissolution pulses is due to the rapid dissolution of surface fines which are created during the surface cleavage process. Extremely small surface fines have a higher solubility than the bulk material, this being a thermodynamic effect related to their small radii of curvature (see discussion in Parks, 1990, for example). It is interesting to note that several of the samples that were hydrolyzed at 100°C were rehydrolyzed one more time, and in some cases, once again (at the same pH and temperature). Even though the magnitudes of the initial release rate pulses decreased with each successive run, they were always present. This suggests that the dissolution of surface fines is not the sole reason for the initially rapid release rates (see Fig. 6a for a surface largely devoid of surface fines after two successive dissolution runs). Another important point is that the complete dissolution of surface fines should be a congruent process. However, the number of moles of Na, Al, and Si released with each pulse was not equal, as can be seen by comparing the maximum rates of Na and Si release in Fig. 7.

It is interesting to note that the occurrence of a prominent spike in the initial release rates appears to be a function of temperature and pH. At 300°C and at acid and neutral pH conditions, the spikes in the Na and Si release rate curves were present but not very pronounced when compared to those at 200 and 100°C. There may be several reasons for this behavior. It cannot be excluded that the initial Na and Si release rates were rapid enough at 300°C that the signal at $t = 0$ was 'swamped out,' given the sampling frequency of once every minute. Closely related to this may be the effect of a possible time lag associated with $t = 0$ and the start of the experiment (see Experimental Methods and Calculations section). In addition, the lack of large Na spike with respect to Si can be explained by assuming that at 300°C, the rate of H^+-

Na^+ exchange is roughly equivalent to that of Si hydrolysis. In such a case, one would not expect any significant degree of preferential Na leaching (i.e., equivalent rates of Na and Si release). Examination of the Na and Si rates in Fig. 1c, where their rates are virtually identical (except at the very outset, close to $t = 0$), is possible evidence for this relationship.

At basic pH and 300°C, there was a complete absence of initial Si rate spikes. Instead, the Si rate curves commonly displayed smooth monotonic increases over an extended period of time, followed by a subsequent leveling-off to constant, steady-state values (Figs. 4c, 5c). This behavior is most probably a real phenomenon, and is probably not due to the manner in which sampling was conducted. The initially depressed values of Si release close to $t = 0$ are perhaps indicative of the inhibition of Si hydrolysis. Potential reasons for this behavior are presently not understood. This phenomenon merits investigation in greater detail in the future.

Progression of the Reaction Front into the Structure

As ions and molecules are rapidly detached from the surface, a reaction front begins to advance into the structure. This reaction front is characterized by the influx of reactant molecules from the solution into the structure. The reason such a phenomenon occurs during the dissolution of feldspars, as well as with many other multioxide silicates, is due to the fact that the initial rates of release of each element from the structure are not identical. The preferential (i.e., faster) release of certain elements leads to preferential leaching of the structure, thereby creating leached layers with a distinctly different chemical composition from that of the bulk. Albite leached layers can be defined in terms of the differential rates of release of Na, Al, and Si; the preferential leaching associated with the two elements that are released at the fastest rates defines two chemically distinct leached layers with different depths. At nearly all pH and temperature conditions in this study, Na was released at a faster rate than both Al and Si, thereby leading to the formation of Na-leached layers. At acid and neutral pH conditions, Al was released at faster rates than Si, leading to formation of Al-leached layers. However, at basic pH, Al and Si were either released congruently, or alternatively, differential rates of Al and Si release led to the creation of either Al- or Si-leached layers.

The advance of the reaction front is defined by the furthest advance of solution species (H^+, H_3O^+, Cl^-, H_2O, K^+, OH^-) into the structure. At acid pH, this corresponds to the maximum depth of H ion penetration, this theoretically equaling the depth of Na leaching, since Na^+ cannot be released until it is exchanged with H ion. At basic pH, the advance of the reaction front can be defined by the furthest depth of penetration of KOH, since K^+ is probably exchanged with Na^+. Even though no direct evidence exists for this ion exchange reaction, the results from a similar study suggest that it is likely. From the results in Hellmann et al. (1990), there is XPS evidence for the presence of Ba^{2+} to depths (500 Å) corresponding to that of Na^+ leaching in an albite that was dissolved (225°C) at basic pH in an aqueous $Ba(OH)_2$ solution.

The influx of hydrolyzing species (H^+, H_3O^+, H_2O, OH^-) associated with the advance of the reaction front and ion exchange reactions results in the concomitant hydrolysis of Al-O and Si-O bridging bonds within the structure. However, since the hydrolysis of these bridging bonds is much slower than ion exchange, the depths of Al or Si preferential leaching should be less than the depths of Na preferential leaching. This is confirmed by the fact that the rate curves in Figs. 1–5 show that Na is initially released at faster rates than Si and Al. The more pronounced differences in release rates at 100°C suggests that the relative difference in the rates of ion exchange and hydrolysis depends strongly on temperature.

Monotonic Decrease in the Rates: Acid pH

The initial rate of advance of the reaction front from the surface region into the bulk structure is very rapid, as are also the initial rates of release of Na, Al, and Si. Each of the release rates passes through a maximum and then starts to decrease monotonically, until a minimum is reached, defined by where the rates become constant (transition A → B → C in Fig. 7). This type of behavior was common to almost all of the experiments in the present study (exceptions to this are discussed further on). A very similar trend was noted for the rate of proton consumption (Fig. 8). Note that the maximum and minimum are uniquely defined as a function of time for each of the elemental rate curves. The observed decreases in the rates of release are a function of several factors. Below, two arguments are presented, one based on diffusion, the other on Al adsorption.

The diffusion argument is based on the rates of diffusion of reactant species in the direction of advance of the reaction front, as well as the rates of product species diffusing in the opposite direction, towards the solid/solution interface. The key to this argument is a feedback relationship between the diffusional fluxes and the rate of retreat of the solid/solution interface (see discussions by Chou and Wollast, 1984, 1985a; Pačes, 1973; Correns and von Engelhardt, 1938).

This feedback relationship is first presented with respect to the influx of reactants into the structure. Examining the B → C transition at acid pH (Fig. 8), two processes may be responsible for the observed decreases in the rate of H^+ consumption and the inward flux of H^+ (i.e., rate of advance of the reaction front). H^+ consumption and the penetration of H^+ into the structure are two interdependent processes, since the advance of the reaction front by H^+ is coupled to consumption by ion exchange and hydrolysis reactions. The flux J_{H^+} into the structure can be expressed in terms of Fick's first law, $J = Ddc/dx$. One factor which serves to decrease the flux J_{H^+} is the decrease in $|-d[H^+]/dx|$ with increasing depth of penetration x. In addition, the coefficient of diffusion D will decrease as H^+ species, initially diffusing through the open surface structure, encounter a more closed structure associated with that of unaltered albite. However, the flux J_{H^+} will only decrease to a point where it equals the rate of retreat of the solid/solution interface. The rate of retreat is of course governed by the element with the slowest rate of release (in expt. B, this corresponds to the rate of Si release). Once a balance between the two processes is achieved, the rate of advance of the reaction front is equal to the rate of retreat of the solid/solution interface. A constant depth of H^+ advance also corresponds to a steady-state depth of preferential Na leaching, since Na^+ and H^+ are an ion exchange couple (region C in Fig. 7). It should be noted, however, that the steady-

state consumption of H^+ (region C, Fig. 8) is not only a function of ionic exchange, but also Al-O and Si-O hydrolysis reactions within the leached zone. Thus, at acid pH, the amount of H^+ consumed will be greater than the amount of Na released (results in Part III, Hellmann et al., 1995).

The same argument can be applied to the outward diffusion of product species. At acid pH conditions, for example, the penetration of H^+ into the structure continuously leaves a more open structure behind the advance of the reaction front. This allows the large scale influx of reactant molecules into the leached layer, thereby increasing the population of Al and Si groups susceptible to hydrolysis reactions. If one takes the case of Al being preferentially leached (expt. B), the outward flux of Al can be expressed in terms of $J_{Al} = Ddc/dx$. As dissolution progresses, $d[Al_{aq}]/dx$ steadily decreases, until a point is reached where the rate of retreat of the solid/fluid interface equals the rate of advance of the Al depleted zone. Several studies, in particular those by Muir and Nesbitt (1991) and Shotyk and Nesbitt (1992), show data which support the idea that Al diffusion gradients influence the rates of dissolution and the thickness of Al leached layers in plagioclase feldspars. However, the influence of aqueous Al on the rates may have been due to other reasons aside from changes in the Al diffusion gradient, as discussed next.

Aluminum adsorption may also play a role in decreasing the release rate of Si and therefore, the fluxes of Na and Al, as well. Even though there is controversy with respect to whether aqueous Al influences the overall rates of feldspar dissolution (Burch et al., 1993), many studies in the literature suggest that Al adsorption does have an inhibitory effect (Chou and Wollast, 1985a; Amrhein and Suarez, 1992; Oelkers et al., 1994). The data from the present experiments do not allow the Al-adsorption hypothesis to be tested. However, data in the literature on the inhibitory effects of Al do leave open the possibility that adsorption reactions within the leached zone and at the surface occur in conjunction with the preferential release and outward diffusion of free Al species.

The adsorption of Al on silica surfaces (i.e., at silanol sites) has been extensively investigated (see, e.g., Dugger et al., 1964; Vydra and Galba, 1967; Allen and Matijevic, 1969, 1970, 1971; Matijevic et al., 1971; Iler, 1973; for a review, see Iler, 1979). Al adsorption on silanol groups on hydrated silica gel surfaces can be represented as a two step, cation exchange process (see Dugger et al., 1964):

$$\equiv\text{Si-OH} \Rightarrow \equiv\text{Si-O}^- + \text{H}^+ \qquad (2a)$$

$$\equiv\text{Si-O}^- + \text{Al}^{3+}\cdot 6\text{H}_2\text{O} \Rightarrow \equiv\text{Si-O-Al}^{2+}\cdot 6\text{H}_2\text{O}. \qquad (2b)$$

The adsorption of Al can alternatively be expressed in terms of a condensation reaction (Allen and Matijevic, 1971):

$$\equiv\text{Si-OH} + \text{Al(OH)}^{2+}\cdot 5\text{H}_2\text{O} \Rightarrow \equiv\text{Si-O-Al}^{2+}\cdot 5\text{H}_2\text{O} + \text{H}_2\text{O}. \qquad (3)$$

Adsorption of Al on SiOH starts at about pH 2.5 at 25°C (Vydra and Galba, 1967), with the adsorption edge located at approximately pH 4–5. According to the results of Dugger et al. (1964), the ion exchange reaction (Eqn. 2a,b) is favored by increasing temperature. The adsorption edge should, therefore shift to lower pH with increasing temperature. This is in part a function of the pK_{a1} and pK_{a2} of Si-OH decreasing, by an amount possibly related to the decrease in the ionization constant of water with increasing temperature (see Tewari and McLean, 1972). Therefore, as the temperature increases, the proportion of SiO^- groups increases at a given pH, which in turn, increases the adsorption potential for positive Al species.

The above reactions suggest that free Al ions diffusing through leached zones may be adsorbed at silanol sites, either at the surface or within the leached zone. This process may be a mechanism for slowing down the rate of Si hydrolysis during the initial stages of dissolution. If Al adsorption does occur, then the establishment of steady-state conditions requires a balanced interrelationship between the rate of Al hydrolysis, Al adsorption, and the rate of release of Si, which in turn, directly controls the rate of retreat of the solid/fluid interface. In addition, it should be noted that Al adsorption on silanol sites may also play a catalyzing role in Si-OH condensation reactions (Casey et al., 1988).

Attainment of Steady State: Acid pH

The establishment of steady-state conditions is dependent on the attainment of a steady-state balance of reactions that serve to open up leached structures and promote the overall dissolution process (ion exchange, hydrolysis of Si-O-Si and Si-O-Al bonds) and those reactions that serve to slow down the overall dissolution process (Al adsorption on silanol groups) and restrict (or reduce) the transport properties of the leached structure (repolymerization reactions of Si-OH groups). The attainment of steady-state conditions of dissolution can be represented by region C in Figs. 7 and 8. This represents both a minimum and a steady state in the rates of release of Na, Al, and Si, as well as the rate of H^+ consumption. This initial steady-state region is important for two reasons: first, it marks a period of dissolution characterized by rates of release that remain constant over an extended period of time; secondly, it is generally characterized by congruent dissolution. Congruency of the reactions may, however, already occur before the attainment of these plateau rates.

In some cases, the initial steady-state rates that were recorded appeared to be transient, as evidenced by smooth, monotonic increases in the rates of Si and Na release over time, up to a point where new and constant steady-state rates of release were achieved. This type of behavior was most noticeable in the acid pH range, especially at 200 and 300°C (see Figs. 1b,c, 2b,c). This effect was less pronounced at neutral pH, and absent in the basic pH range. Recasting Fig. 1b (pH 2.0 and 200°C), by using a linear rate ordinate, more clearly shows the gradual increase in Si and Na rates (labeled as transition C → D; Fig. 9). The exact same type of behavior shown in Fig. 9 was noted for three different dissolution experiments at the same conditions. It is also interesting to note that the rate of change in the steady-state rates occurred much faster at 300 than at 200°C, as can be seen by a comparison of the rate curves in Figs. 1b,c and 2b,c.

Based on dissolution experiments at relatively similar conditions (pH 0.7 and 225°C), the consumption of H^+ as a

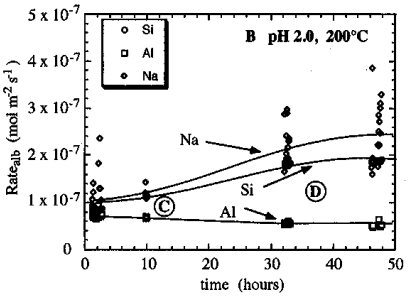

FIG. 9. The evolution of the steady-state rates of release of Na, Al, and Si at pH 2.0 and 200°C (adapted from Fig. 1b). These rate data also represent the continuation of Fig. 7 (indicated curves are schematic). The increase in the rates of Si and Na and the attainment of new steady-state rates (trend C → D) are postulated to result from a "structural re-equilibration" of the initially formed leached layers. The divergence of the Al rate curve is probably due to precipitation. Note that the increase in the Si and Na rates is qualitatively similar to the proton consumption trend C → D shown in Fig. 8.

function of time shows a very similar trend, as shown by transition C → D in Fig. 8 (data from Hellmann et al., 1990). The transition C → D is characterized by an increase in H^+ consumption by a factor of 6.5 over a 2 h period of time, beyond which the curve remains constant. It should be noted that only a qualitative comparison between the two datasets is possible since the experimental conditions were not the same.

The evidence above suggests that particularly at acid pH conditions, the evolution of the release rates is quite complex and may continue well beyond the time period associated with the initial attainment of congruent, steady-state release rates. At this point, one cannot exclude the explanation that the observed increases in steady-state rates were due in part to an increase in the effective surface area, due mainly to the creation of etch pits, etc. (see discussion in Stillings and Brantley, 1995). However, the fact that these increases in rates were pH dependent seems to indicate that another mechanism is responsible for this. An alternative explanation, based purely on conjecture at this point, is based on a "structural re-equilibration" process occurring within the leached layers, at a slower timescale than that associated with the initial formation of the leached layers. Restructuring of the leached layers necessarily would cause a readjustment of the fluxes of reactants diffusing towards the fresh albite/leached zone interface (H^+ in Fig. 8) and product species being transported towards the surface/solution interface (Na and Si in Fig. 9). Unfortunately, since the interdependence of all of the forward, parallel, and backward reactions is not known with sufficient detail, the resolution of this problem is not yet possible.

Depths of Preferential Leaching

The depths of preferential leaching were based on the integration of each elemental rate curve (using linear rate scales) associated with a given temperature and pH condition. Since the Na, Al, and Si release rates were normalized with respect to the stoichiometry of albite, the integral of each rate curve yielded the moles (n) of albite dissolved, calculated with respect to a given element. The integration limits extended from $t = 0$ to $t = t(f)$, which corresponded to where the rate curves converged (i.e., convergence of Na and Si or Al and Si rates). Leaching depths were solely based on the initial convergence of the rate curves during the first stages of dissolution; any subsequent changes in the rate curves were not considered (as in Fig. 9).

The preferential depth of leaching d was calculated using the following formula

$$d = \Delta\text{mol} \times 100.07\ \text{cm}^3\ \text{mol}^{-1} / (0.013\ \text{m}^2\ \text{g}^{-1} \times \text{avg. mass}), \quad (4)$$

where 100.07 $cm^3\ mol^{-1}$ is the molar volume of albite (Robie et al., 1984). As an example, the depth of preferential leaching of Na with respect to Si is proportional to $\Delta\text{mol} = n\text{alb}_{\text{Na}} - n\text{alb}_{\text{Si}}$, and similarly, the depth of preferential leaching of Al with respect to Si depends on $\Delta\text{mol} = n\text{alb}_{\text{Al}} - n\text{alb}_{\text{Si}}$ (note that the molar difference Δmol is stoichiometrically normalized). If, however, the difference in the latter case is a negative quantity, then this implies the preferential release of Si with respect to Al.

It is important to note that depths calculated from solution data and the application of Eqn. 4 are not directly comparable to depths obtained directly from depletion profiles derived from surface analytical techniques (for the same conditions of dissolution). The calculated depths of preferential leaching (using Eqn. 4) assume that a given leached layer is modeled by a step-like boundary representing the transition from a zone of complete depletion to a zone of non-depletion. In reality, of course, the depletion of an element is characterized by a concentration gradient. If a linear gradient is assumed, for example, then the depths calculated from solution analyses (Eqn. 4) are multiplied by a factor of 2. In the present study, the leaching depth results are presented in the context of a linear gradient. Most commonly (see the XPS profiles in Hellmann et al., 1990, for example), depletion profiles have a sigmoidal form that show a gradual, asymptotic approach to the bulk composition, represented by a calibration curve that is representative of fresh, unaltered material. These types of profiles inherently produce depths of depletion that are considerably greater than other types of profiles. Therefore, leaching depths are strongly dependent on the nature of the depletion profile. In addition, the use of Eqn. 4 does not take into account structural changes occurring within the leached zone. Experimental evidence suggests that leached zones have an amorphous-like structure (Casey et al., 1989; Petit et al., 1990; Hellmann et al., 1990; see also discussion on diffusion coefficients further on). This implies that the molar volume term in Eqn. 4 should not be treated as a constant, but rather should be a function of the depletion gradient(s) within the leached zone.

The determination of leaching depth estimates was not always straightforward. The Na and Al rate curves at 100°C generally did not converge with the Si curves (see Fig. 1a, for example). Instead of eventually converging, as would be expected for the onset of steady-state, congruent dissolution conditions, the rate curves became parallel. One can hypoth-

esize that either true steady-state conditions were not achieved, or analytical inaccuracies (Na and Al) prevented the convergence of the rate curves. Taking the case of dissolution at 100°C and pH 2.0 (Fig. 1a), the calculated depth of preferential Na leaching would be > 6840 Å if it is assumed that the nonconvergence of the Na and Si rate curves is in fact a real phenomenon. On the other hand, if analytical uncertainties are assumed, then the Na and Al rate curves can be "corrected" by a forced convergence with the steady-state Si rate. This was done by modifying each individual rate (data point) by the same amount, such that the entire rate curve was shifted. Referring again to the 100°C, pH 2.0 rate curves, when the Na rate curve was shifted (downward), the Na and the Si rate curves converged at $t = 1.5$ h ($t = 1.5$ h is the time when the curves became roughly parallel). After correction, the calculated depth of Na leaching over this time period was 1379 Å. Even though neither hypothesis can be proven at this point, it was decided to calculate leaching depths that err on the conservative side.

Sodium-leaching depths

Leached layers depleted in Na developed at nearly all pH and temperature conditions in the present study. Calculated depths are listed in Table 1, and average depths are shown graphically in Fig. 10. The estimated accuracies of the leached layers (±20–30%) depend not only on the limits of integration that were chosen for each rate curve, but also on the uncertainties associated with the rates. There was admittedly an arbitrary nature in the choice of the upper limits of integration for each set of rate curves. Unfortunately, this problem cannot be easily avoided with this type of data analysis.

Leaching depth estimates for the same conditions of dissolution often varied by an order of magnitude. For example, Na leaching depths at pH 2.0 and 300°C ranged from 151–1405 Å (Table 1). This large variation in depths is apparently a real phenomenon and cannot be attributed to the methods used in calculating the depths. Leaching depths differing by an order of magnitude were also reported by Rose (1991) for albite samples dissolved at 100°C at the same pH. Sample heterogeneity is the most probable cause for this. These results point out the importance of the overall trends observed, and not individual leaching depth estimates.

To summarize the pH dependency of the Na leaching depths from the present study, the greatest depths were determined at acid and basic pH; they exceeded those at neutral pH by roughly an order of magnitude. The decrease in depths with increasing pH in the acid to neutral pH region is unambiguous and is in accord with other dissolution studies at low and elevated temperatures (Chou and Wollast, 1985a; Holdren and Speyer, 1985; Muir et al., 1989; Casey et al., 1989; Petit et al., 1990; Hellmann et al., 1990). The transition in dissolution conditions from neutral to basic pH generally resulted in an increase in leaching depths; however, the variation in the calculated depths precludes the establishment of an unambiguous trend. The lack of a trend in the basic pH region can also be extrapolated from data in Chou and Wollast (1985a). Despite the large variation in depths in the present study, it is important to note that these results demonstrate that Na leaching does occur to quite significant depths at basic pH and elevated temperatures.

The pH dependence of leaching depths implies that ion exchange reactions are quantitatively more important at low and high pH conditions than at neutral pH. This follows as a consequence of the pH-dependent concentration gradients controlling the rates of inward diffusion. Thus, $|-d[H^+]/dx|$ increases with decreasing pH in the neutral to acid pH region, and likewise, $|-d[K^+]^*/dx|$ increases with increasing pH in the neutral to basic pH region *(the cation is of course dependent on the base used). This relationship predicts that maximum depths of leaching and penetration of hydrolyzing species should occur at acid and basic pH conditions. Taking this one step further, this implies that the overall dependence of dissolution rates on pH is in part related to the structural and transport properties of the leached layers.

The dependence of leaching depths on temperature could not be determined from the data in this study, and therefore, the leaching depth-temperature relations shown in Fig. 10 should not be over-interpreted. Far more replicate analyses would have to be carried out in order to establish an unambiguous relationship between temperature and leaching depth at any given pH. Nonetheless, the data in Fig. 10 reveal that the leaching depths do not show a dramatic increase with increasing temperature (at pH 2.0, there was an apparent decrease). This can be attributed to the interdependency between the rates of diffusion and hydrolysis in determining leaching depths. In general, the activation energy of diffusion is less than that of hydrolysis (Lasaga, 1981). Therefore, rates of diffusion will increase more slowly with temperature than rates of metal-oxygen bond hydrolysis. As mentioned earlier, if the two rates are equal, there should be no preferential leaching.

Aluminum-leaching depths

Even though Al-leaching depths were often not determinable at higher temperatures due to the precipitation of an Al phase, the overall results from this study show that Al was preferentially released with respect to Si under acid and neutral pH dissolution conditions. Under mildly basic pH conditions (pH < 10 at 25°C), the degree of preferential release of Al or Si generally was minor, such that dissolution can be considered to be more or less congruent. At intermediate basic pH conditions, dissolution was either congruent, or alternatively, Al or Si was preferentially released. At more extreme basic pH conditions at 200 and 300°C (pH ≥ 12 at 25°C), only Al was preferentially released, to significant depths. In general, the Al depths were an order of magnitude less than the corresponding Na depths of depletion. The Al leaching depths determined in this study are shown in Table 1. As was the case for Na leaching depths, the estimated accuracies are on the order of ±20–30%.

The results at 100°C from the present study show a decrease in the depth of Al leaching with increasing pH in the acid to neutral pH range. This trend is in accord with results from previous feldspar dissolution studies, both at 25°C and at elevated temperatures (Chou and Wollast, 1984, 1985a; Casey et al., 1989; Muir et al., 1990; Hellmann et al., 1990). It is not clear at this point if the overall lack of a trend in the pH dependency at basic pH conditions is the result of insufficient data (mainly due to precipitation reactions), or whether it is

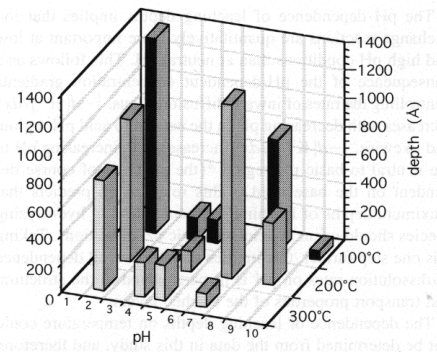

Fig. 10. The average depths of Na leached layers (estimated accuracy 20–30%) as a function of pH and temperature. The essential trend is that of decreasing depth of leaching with increasing pH in the acid to neutral pH range. No unambiguous trend is apparent in the basic pH range. There appear to be no dramatic increases in the leaching depths with temperature (note the decrease at pH 2.0). The establishment of definitive trends for depth vs. temperature requires more data however.

due to the interplay of processes not yet understood. The presumed complexity of dissolution at basic pH conditions may be due to the changing speciation of Si-OH and Al-OH groups within the leached zones, this being a function of both temperature and pH (see discussion below). Nonetheless, the present results in conjunction with XPS results from a previous study (Al depletion to a depth of 455 Å at pH 7.7, 225°C; Hellmann et al., 1990) point out that significant leaching of Al can take place at basic pH conditions. This stands in contrast to previous results at 25°C, which show that Al and Si release rates are essentially congruent at basic pH (Chou and Wollast, 1984, 1985a; Holdren and Speyer, 1985; Casey et al., 1989).

Leached Layers and Speciation of Si-OH and Al-OH Groups

The formation of leached layers at high temperature (results from the present study and Hellmann et al., 1990), as well as at 25°C (Chou and Wollast 1984; Holdren and Speyer, 1985; Muir et al., 1990; Casey et al., 1989), can be examined in the context of surface speciation. Based on numerous surface titration results in the literature, the charge of surface metal hydroxyl groups is related to the solution pH. Blum and Lasaga (1988) showed that the surface charge of albite is directly related to the overall dissolution rate r, such that at 25°C: $r \propto c_{\text{S-OH}_2^+}^{1.0}$ at pH < 6 and $r \propto c_{\text{S-O}^-}^{1.0}$ at pH > 7 (where $c_{\text{S-OH}_2^+}$ and $c_{\text{S-OH}^-}$ represent the surface concentrations of metal-OH_2^+ and metal-OH^- groups, respectively; note also that S-OH^- is equivalent to S-O^- in the following discussion). In order to interpret the preferential leaching results in the present study, an argument based on surface speciation is applied to metal hydroxyl groups within the leached zones. This approach is based on the premise that charged metal hydroxyl groups are preferentially hydrolyzed with respect to neutral groups. It is implicitly assumed that the chemical characteristics of metal hydroxyl groups (≡S-OH) found within a leached layer are identical to those occurring at the surface (despite the lack of experimental evidence confirming this).

At 25°C, Si-OH has the following acid/base constants; $pK_{a1} \approx -2.0$ and $pK_{a2} = 6.6$ (amorphous SiO_2; pK_{a2} averaged from Schindler and Kamber, 1968, and Sigg, 1973); for Al-OH, $pK_{a1} = 7.3$ and $pK_{a2} = 9.8$ (Al_2O_3 used; Hohl and Stumm, 1976, and Kummert and Stumm, 1980). Therefore, Si-OH is the dominant silanol group at pH < 6.6, whereas the negatively charged Si-O^- group dominates at pH > 6.6. With respect to Al-OH speciation, Al-OH_2^+ is the dominant aluminol group at pH < 7.3, Al-OH is dominant at $7.3 <$ pH < 9.8, and Al-O^- is dominant at pH > 9.8. As temperature increases, the pK_a values do not remain constant, and therefore, the speciation of silanol and aluminol groups will change as well. The determination of speciation at temperature requires the calculation of pK_a values as a function of temperature. For conditions ranging from 100–300°C, such calculations are non-trivial (due mostly to a lack of thermodynamic data) and are therefore beyond the scope of this paper.

It is generally accepted that pK_a values decrease with increasing temperature (see, e.g., results from Tewari and McLean, 1972; Brady, 1994). There is experimental evidence that the change in the pK_a is a function of the change in the ionization constant of water (pK_w) (see Tewari and McLean, 1972). To illustrate this point, the evolution of the pH_{zpc} of Al_2O_3 ($pH_{zpc} = (pK_{a1} + pK_{a2})/2$) with temperature is calculated, using a 1 pK_a model and the application of the van't Hoff equation:

$$d\log K_H/dT = (dpH_{zpc}/dT)_c = \Delta H_{\text{ads H}^+}/2.303RT^2, \quad (5)$$

where K_H is the equilibrium constant for proton adsorption at the pH_{zpc}, C refers to the electrolyte concentration, and $\Delta H_{\text{ads H}^+}$ is the isosteric heat of proton adsorption at the pH_{zpc} (see application in Macheski and Jacobs, 1991). Using this method yields the following approximate pH_{zpc} values: 8.5 (25°C), 7.0 (100°C), 5.5 (200°C), 4.8 (300°C). As a comparison, at 300°C (sat. vapor pressure), the value of pK_w is 11.4 (Marshall and Franck, 1981). Similar calculations for Si-OH are not possible due to a lack of thermodynamic heat capacity data (i.e., $\Delta H_{\text{ads H}^+}$ for Si-OH). To circumvent this problem, the temperature dependence of the acid/base properties (i.e., pK_a's) of both Si-OH and Al-OH groups are simply approximated by the temperature dependence of pK_w.

At acid pH conditions, Si-OH and Al-OH_2^+ groups should predominate at all temperatures (25–300°C). Given that the Al groups are charged, this should lead to their preferential release from sites both at the surface and from within the structure. This differential reactivity is based on surface titration results (Blum and Lasaga, 1988) as well as ab initio calculations (Xiao and Lasaga, 1994). This prediction is in accord with the results from the present study, where Al was always preferentially released with respect to Si at acid pH conditions. At neutral pH conditions, Si-OH and Al-OH/Al-OH_2^+ groups are predicted to predominate at 25–100°C. The slight predominance of positively charged Al groups is probably the reason why there is evidence for the preferential release of Al even at neutral pH, even though the degree of preferential release should be very modest. At 25°C, Al leached layers of no more than 10–20 Å have been found

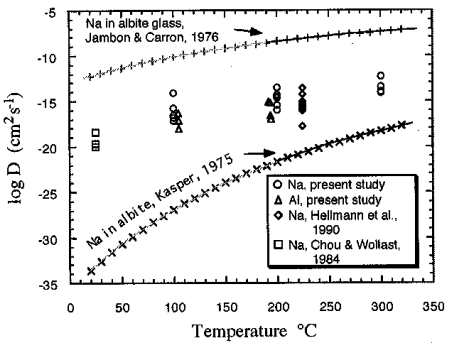

FIG. 11. Diffusion coefficients for Na and Al diffusion through leached layers (based on steady-state conditions and constant leached layer thicknesses) from data in the present study, Hellmann et al. (1990), and Chou and Wollast (1984). The curves are representative of experimentally measured Na diffusion coefficients in albite and albite glass (from the literature). The fact that the leached layer diffusion coefficients fall between the two curves suggests that the leached layers are structurally more open than crystalline albite. Note that the extrapolation of the 2 curves below 200°C may not be accurate (stippled curve pattern).

(note, in many studies, no preferential leaching was observed). At 100°C, the degree of Al leaching was minimal in the present study (see Table 1); this is also in accord with the predicted predominance of Si-OH and Al-OH/Al-OH_2^+ groups (at higher temperatures, Al leaching depths could not be determined due to Al precipitation).

With increasing pH at basic pH conditions (at 25°C), the distribution of Si groups is predicted to change in favor of the predominance of Si-O^- groups, starting at pH > 6.6. The predominance of Al-O^- groups is predicted to occur at pH > 9.8. In many of the cited studies at 25°C (see discussion above), Si and Al were observed to dissolve congruently and no leached layers were observed. The results of Chou and Wollast (1984) indicate that the preferential leaching of Al or Si is possible, depending on pH. Even so, their results show that these leached layers are insignificant (≤10 Å) at mildly basic pH conditions. With increasing temperature or increasing pH, it is expected that speciation should shift from SiO^- and mixed Al-OH/Al-O^- groups to the exclusive predominance of negatively charged Si-O^- and Al-O^- groups. This may explain the shift from insignificant preferential leaching of Al or Si to significant Al leaching at very elevated pH conditions, where depths of Al leaching ranged up to several hundreds of Å (see Table 1, and results in Hellmann et al., 1990).

Therefore, based on the available data at 200 and 300°C, it seems reasonable to suggest that in the pH range where negatively charged Si-O^- and Al-OH/Al-O^- groups predominate, either Al or Si are preferentially released (to insignificant depths, see Table 1). The pH range where there is a predominance of both Si-O^- and Al-O^- groups occurs at very basic pH conditions. Even when taking into account errors in the speciation calculations, it is likely that at 200 and 300°C and pH 12.0 (pH meas. at 25°C), that both Si-O^- and Al-O^- groups predominate. Under such conditions, Al was always preferentially hydrolyzed, with significant depths of preferential leaching (hundreds of Å). This may be due to the fact that when both negatively charged silanol and aluminol groups are present, the differences in negative charge density of the Al-O^- and Si-O^- groups may play a minor role in the preferential hydrolysis of Al.

Alternative explanations need to be briefly considered to explain the results. One such reason may be related to the fact that Al-O_{br} bonds are longer than Si-O_{br} bonds (where O_{br} denotes a bridging O) (Harlow and Brown, 1980; Geisinger et al., 1985). This implies that Al-O bonds are intrinsically weaker and should, therefore, be more easily hydrolyzed. In addition to these length differences, MO calculations (de Jong and Brown, 1980) suggest that the reactivity of O_{br} sites is greater in Al-O_{br} linkages than in Si-O_{br} linkages (see discussion in Hellmann et al., 1990). This result was substantiated in recent ab-initio simulations of dissolution, whereby it was shown that Al-O_{br} linkages are preferentially hydrolyzed with respect to Si-O_{br} linkages (Xiao and Lasaga, 1994). Thus, the greater reactivity of Al-O bonds may explain the observed preferential release of Al at very high pH.

Diffusion in Leached Layers

The determination of diffusion coefficients allows for the estimation of Na and Al diffusion rates through the leached layers. Since the true nature of the depletion gradients could not be determined from the data, a linear depletion gradient and a constant diffusion coefficient were assumed. Fick's first law of diffusion is used to calculate the coefficient of diffusion D.

$$J = D\frac{dc}{dx}, \tag{6}$$

where J is the flux (equal to the rate of Na or Al release), dc is the change in concentration of Na or Al (assumed to be zero at the solid/solution boundary and 0.01 mol/cm³ at the leached zone/fresh albite boundary), and dx is the distance of diffusion, which is equal to the depth of leaching (from Table 1). The fluxes used in the calculations were based on the rates of release where the Na and Al rate curves became coincident with the respective Si rate curves (as was the case for the determination of leaching depths).

Figure 11 shows the values of log D for Na and Al determined from this study, as well as log D_{Na} at 225°C from Hellmann et al. (1990) and log D_{Na} at 25°C from Chou and Wollast (1984). For the sake of comparison, linear diffusion gradients were applied to each set of data. The log D values plotted in Fig. 11 are bounded by two curves representing the temperature dependence of log D for the diffusion of Na through albite and albite glass. The curves were calculated using an Arrhenius equation:

$$D = D_0 \exp(-Q/RT), \tag{7}$$

The pre-exponential factor (D_0) and activation energy (Q) values were obtained from Smith and Brown, 1988 (Tables 16.1 and 16.3; based on original data reported in Kasper, 1975 (albite) and Jambon and Carron, 1976 (albite glass)). The variation in the log D values obtained at any one set of tem-

perature and pH conditions in the present study is perhaps due to the heterogeneity of the samples, such that the overall D measured for any given sample is a function of volume diffusion as well as grain boundary diffusion.

In Fig. 11, several observations are immediately noticeable. First, the calculated log D_{Na} values at all temperatures (25–300°C) are delimited by the log D_{Na} values for albite and albite glass. This is potentially indicative that diffusion through the leached layer occurs within an altered structure that has transport properties intermediate between those of crystalline albite and albite glass (the glass structure consists of 6-membered rings; Taylor and Brown, 1979). This is a consequence of the preferential leaching of Na and Al leaving behind a structure that is much more open and porous than crystalline albite. The second observation is that the log D_{Al} values generally are within the same order of magnitude as the corresponding values for Na (also observed in Hellmann et al., 1990). However, in crystalline albite (and presumably in albite glass, as well), the rates of self-diffusion measured for Na are several orders of magnitude greater than for Al (Smith and Brown, 1988). At this point, the data are not sufficient enough to determine whether the phenomenon of similar diffusion coefficients is real or not. It may point to a diffusional process occurring in an open structure where differences in the charge and size of the diffusing species play a less significant role (as in a liquid) than would be the case for diffusion in a crystalline solid (noting that it is presumed that Na diffuses as Na^+ and Al as $Al(OH)_{4-n}^{n-1}$, where n varies from 0–4, depending on pH).

Given the fact that the exact structural nature of the leached layers is not known, the data do not allow one to test whether the depths of preferential leaching are in fact limited by the rates of diffusion of Na and Al (with reference to the feedback model discussed earlier). As an example, if the leached layers are modeled as albite glass, then the values for log D obtained from the rate data should coincide with those measured in glass diffusion experiments. Nonetheless, it should also be remembered that the diffusion coefficients are based on conservative estimates for leaching depths; the true leaching depths are probably much greater (see discussion in Depths of Preferential Leaching).

Another observation, shown in Fig. 12, pertains to the relationship between the diffusion coefficients and pH (all calculations based on a linear diffusion gradient). The calculated log D values decrease with increasing pH in the acid to neutral pH range. This relationship was also shown to be true for data obtained at 225°C (Hellmann et al., 1990), as well as at 25°C (Chou and Wollast, 1984). Even though the data in the basic pH range (from the present study) are sparse, it appears that with increasing pH, the log D values increase from neutral to basic pH (verification of this trend would require more data). The inverse relationship between log D and pH (acid to neutral pH conditions) is probably due to several factors. One possible factor may be related to the transport properties of the leached structure (i.e., D) as a function of pH. At low pH, the ion exchange of H^+ and Na^+ and the preferential hydrolysis of Al groups from the structure are more significant than at neutral pH. The result of this may be that the leached layers created at low pH are more open and porous than those created at neutral pH conditions. For this reason, the leached layer D values at low pH are significantly greater than those at neutral pH. The importance of this is explored in more detail in the following section.

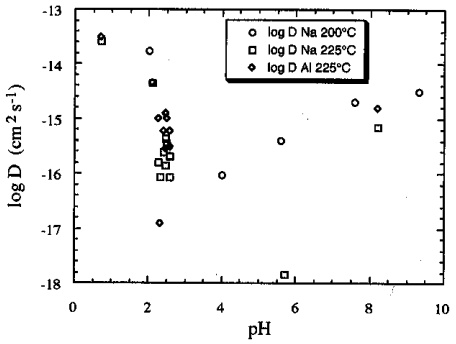

FIG. 12. Leached layer diffusion coefficients for Na and Al at 200 and 225°C. Each set of experimental data shows a strong dependence on pH. Despite the large variation in values at any given pH, diffusion coefficients are generally lowest in the neutral pH range. This implies that leached layers formed at acid and basic pH conditions are more open and porous than those created at neutral pH conditions. The fact that the Na and Al coefficients are of the same magnitude is also evidence for diffusion occurring through an open structure (see text for details).

Structural Interdependence of Sodium, Aluminum, and Silicon Release Rates

The exchange reactions between H^+ (at acid pH) and K^+ (at basic pH) with Na^+ are associated with the influx of aqueous species into the structure (see, e.g., the XPS data in Hellmann et al., 1990). These exchange reactions have the effect of opening up the structure and thereby increasing the number of metal-oxygen bonds which are susceptible to hydrolysis by solvent molecules (H^+, H_3O^+, H_2O, OH^-). This theoretically should accelerate the hydrolysis of Al-O-Si and Si-O-Si bridging bonds within the leached structure.

The observation that rates of diffusion are dependent on the nature of the leached layers is possible evidence for the preferential release of one element influencing the release rates of other elements within the structure. Diffusion of species occurs more rapidly (as evidenced by higher D values; see Fig. 12) through leached layers created at acid pH conditions compared to those created under neutral pH conditions. Thus, under conditions where the preferential release of one or more elements is kinetically favored, one would expect the leached layers to be structurally more open and porous, thereby resulting in faster rates of diffusion. It is hypothesized that this structural interdependence not only controls diffusional fluxes, but also influences the overall dissolution process. The purpose of the following discussion is to examine the nature of this relationship.

In order to investigate this idea of structural interdependence, the number of moles of Na, Al, and Si released during the initial stages of dissolution was determined, based on an integration of stoichiometrically normalized, linear elemental

rate vs. time curves for each set of pH and temperature conditions. The integration limits extended from $t = 0$ to $t = f$, such that the rate $r(f)$ satisfied the following: $\{r(f) - r(f + \delta)\}/r(f) \leq 3\%$; therefore, this covered the time period from the beginning of dissolution to the attainment of initial steady-state conditions (where the slope in the rate curves initially became zero). It is important to note that these integration limits did not always correspond to those used for the calculation of leaching depths, where the upper time limit of integration was based on where the Na and Al rate curves became coincident with the Si rate curve.

As can be seen in Fig. 13a,b, the majority of the Si-Na and the Al-Na data lie below a line representing a 1:1 congruent release ratio, indicating the preponderant release of Na with respect to Al and Si during the initial period of dissolution. The release of network-modifying Na^+ from the structure is positively correlated with the initial release of Al and Si, which are network-forming elements. However, the lack of a clear trend between the moles of Si and Al released as a function of the moles of Na released demonstrates that the degree of correlation is very weak for data representing the entire range of temperature and pH conditions.

The correlation of the data is, however, dependent on temperature. The data at 100°C (Fig. 13a,b) are in particular interesting in that they possibly suggest a complex relationship between Na ion exchange and Si and Al hydrolysis (or, alternatively, there may simply be no correlation!). Contrary to the data at 100 and 200°C, the 300°C Si-Na data show a very clear linear trend (Fig. 13a). This is evidence that there is a direct coupling between ion exchange reactions within the leached zone and the initial, non-steady-state rates of hydrolysis of Si-O-Si bonds. The tendency towards congruency at 300°C (see Figs. 1c, 2c, 3c, 4c) probably occurs since with increasing temperature, the relative difference between the rates of ion exchange and hydrolysis diminish, due to the strong temperature dependence of hydrolysis reactions (attributable to the higher activation energy of hydrolysis reactions). This explanation, however, needs to be substantiated with more experimental data. The relationship between the moles of Al and Na released may be similar to that of Si and Na; however, the temperature dependence of the data could not be analyzed due to the lack of Al data at higher temperatures (due to precipitation reactions).

Figure 13c shows that there is a positive but sublinear relationship between the initial, non-steady-state amounts of moles of Si and Al released. Even though both elements are network formers, the lack of linearity of the data on the log-log plot shows that the release of Si is not directly related to the degree of Al preferential release. One possible reason for this is the role of condensation reactions, whereby adjacent Si-OH groups (created, for example, by the hydrolysis of Al-O-Si bonds) recombine to form Si-O-Si linkages (Pederson et al., 1986; Bunker et al., 1988; Casey et al., 1988, 1989, 1993). This type of structural reorganization of network forming linkages is in fact necessary for maintaining the structural integrity of the leached zones. A leached zone where Al and Si release are directly coupled with each other would not be stable, and would probably collapse, due to a lack of sufficient network forming elements. Another reason for the nonlinearity in the Si-Al release data can be attributed to the speciation

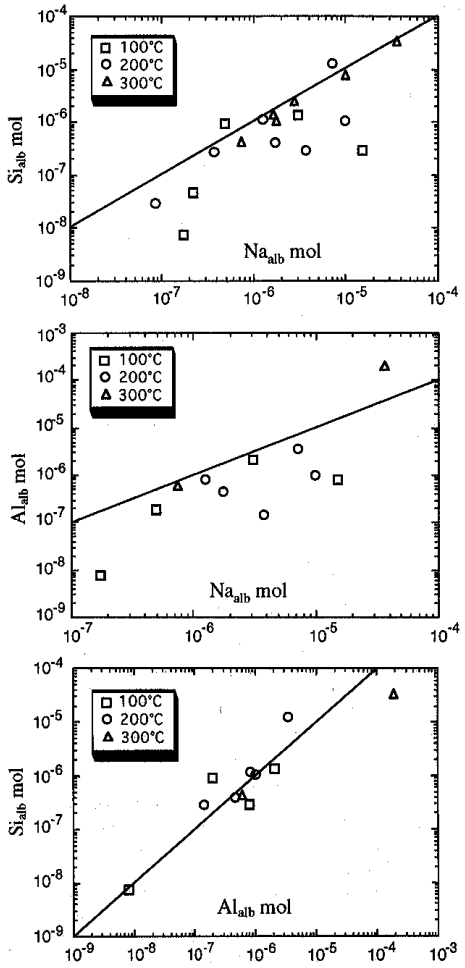

FIG. 13. Relationship between the *pre-steady-state* moles of Na, Al, and Si released for all pH and temperature conditions. The lines in each plot indicate congruent dissolution. (a) and (b) show that the degree of correlation (congruency) between Al and Si release vs. Na release increases with temperature. (c) shows the positive but nonlinear relationship between Si and Al release. These plots show that there is a certain degree of structural interdependence between the release of Na, Al, and Si during the *initial stages* of dissolution when leached layers are formed.

of the Al and Si groups within the leached zones. The pH conditions imposed by the hydrolyzing species present within the leached zones will determine both the speciation of Si-OH and Al-OH groups and their hydrolysis behavior. Depending on the pH, Si-OH, and Al-OH groups may be differently charged, and therefore will be hydrolyzed at different

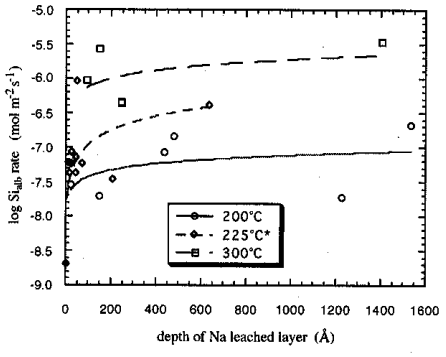

FIG. 14. Steady-state rates of dissolution (using log Si) vs. depths of Na leaching at 200, 225 (data from Hellmann et al., 1990), and 300°C reveal a logarithmic relationship. This nonlinearity indicates that the influence of Na leaching on the rates of Si hydrolysis begins to level-off with increasing depths of Na leaching.

rates (see Blum and Lasaga, 1988; previous discussion above).

Rates of Dissolution and Leached Layer Depths

The relationship between the preferential release of Na and the overall rate of dissolution, as measured by the steady-state rate of Si release, is shown in Fig. 14. In this case, the preferential release of Na is expressed in terms of the depth of Na leaching. Three sets of data are shown: 200 and 300°C from the present study, and data at 225°C from Hellmann et al. (1990). The trends of the log Si rate vs. depth of Na leaching data suggest that a logarithmic relationship exists for each dataset. This nonlinear relationship indicates that the influence of Na leaching on the rates of Si hydrolysis begins to decrease and level off with increasing depth of preferential leaching. A similar plot of Si rate vs. Al leaching depths using data from the present study was not possible due to the problems of Al precipitation. Welch and Ullman (1993) showed that a positive relationship exists between the overall dissolution rate of plagioclase and the degree of Al preferential release.

An interesting relationship between the overall rate of dissolution and Al-leached layer depths can be shown for the plagioclase solid solution series, based on an extrapolation of data at 25°C and pH 2.0 from Casey et al. (1991). This study showed that the rates of dissolution (based on Si) increase as a function of the mol% anorthite (with the exception of the oligoclase and andesine rates). Based on an integration of concentration vs. time curves from this study (Fig. 2, Casey et al., 1991), it was possible to determine depths of preferential Al leaching as a function of plagioclase composition. In addition to the plagioclase data, the dissolution rate of quartz at 25°C and pH 2.1 was utilized (Brady and Walther, 1990). Quartz was chosen as an "endmember" network silicate mineral which does not undergo any preferential leaching reactions during dissolution (R. Hellmann et al., unpubl. data). The resulting correlation between the steady-state rates of Si release and the depths of Al leaching show a logarithmic relationship (see Fig. 15), very much like the ones shown for the dissolution rate vs. Na leaching depth relation shown in Fig. 14. The nonlinear variation of leached layer thicknesses and dissolution rates as a function of plagioclase composition was also shown by Shotyk and Nesbitt (1992) (see also SIMS results regarding depth of leached layers and plagioclase composition in Muir et al., 1990). On the other hand, over a very limited depth range (<30 Å), Brantley and Stillings (1995) extrapolated a linear trend for the relation between dissolution rate and depth of K depletion, based on data in Schweda (1990). Even if the exact relation is not yet known, it is apparent that these results show that mineralogical composition and structure are key parameters in controlling leached layer thicknesses and the overall dissolution rate.

In conclusion, the results above show that when feldspars (and other similar silicates) preferentially lose certain structural elements, the resulting leached layers permit the influx of hydrolyzing species to considerable depths into the structure. The important point is that the depth of leached layers is a controlling factor with respect to the number of Si-O-Si bonds that are available for attack by hydrolyzing species, both at the surface and within the leached structure. This is one likely reason for the noted increase in the overall rate of dissolution as a function of Na- and Al-leaching depths. Another related reason is the fact that the structural openness of the leached layers increases with depth of leaching (results based on diffusion coefficients and depths of leaching), again facilitating both the hydrolysis of metal-oxygen bonds within the structure and the subsequent detachment and removal of hydrolysis products. Of course, the processes invoked above must also include reactions that limit hydrolysis reactions within leached layers. Back reactions, such as those associated with Si-OH condensation reactions, are one example of this. This is probably one of the main reasons for the nonlinearity

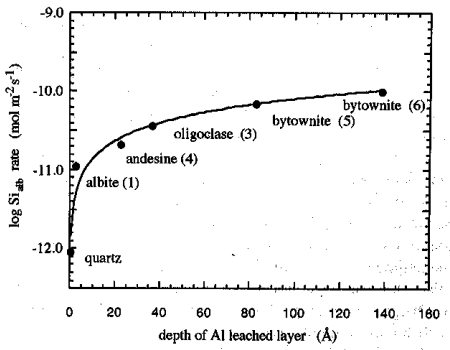

FIG. 15. Log Si rate (normalized to albite) at 25°C and pH 2 vs. depth of Al leached layers in the plagioclase solid solution series. Quartz has been included to illustrate a network silicate mineral which does not form leached layers during dissolution. Note the similarity between this trend and those in Fig. 14. Plagioclase rate data, leached layer depths (extrapolated from Fig. 2), and compositions are from Casey et al. (1991)—note that the numbers in ( ) refer to Table 1 in Casey. Quartz data obtained from Brady and Walther (1990).

(i.e., logarithmic relationship) in the dissolution rate-leaching depth relationships shown in Figs. 14 and 15.

Aluminum Precipitation

Diffusion and sorption

The presence of a secondary precipitate at the mineral/fluid interface may influence the release rates of the individual elements composing the structure. A surface precipitate may act as a diffusional barrier to the outward flux of hydrolysis products, thus slowing down their rates of release to the solution. This can change the rate controlling step of a dissolution process from reaction-controlled to diffusion-controlled.

Based on the experimental evidence in the present study, the effect of surface precipitates was negligible, both with respect to diffusion as well as sorption reactions. The lack of diffusional hindrance is demonstrated by Figs. 1–3, where the release rates of Si and Na remain unaffected by the continuous precipitation of a secondary Al surface phase. Similar results, for much thicker precipitate rinds, are shown in Hellmann et al. (1989). The main reason why diffusion is not hindered is due to the interconnected porosity of the precipitates (see Fig. 6c–f). These results support the empirical Pilling-Bedworth relation (see Gommes and Dekeyser, 1976) which predicts no retardation of outward diffusing species so long as the molar volume ratio of precipitate to reacting mineral is less than unity. In the present experiments, $V_{ppt}/V_{alb} = 0.2$ (where a boehmite precipitate is assumed). In a recent study of silicate weathering, this empirical rule was substantiated (Velbel, 1993).

The presence of surface precipitates with an inherently high surface area, such as shown in Fig. 6c, may be important in terms of sorption reactions at charged sites on the boehmite surface. Given that the pH_{zpc} of boehmite is in the range of 7.7–9.4 (Parks, 1965), the adsorption of negatively charged species should be particularly favored to occur at $pH < pH_{zpc}$. However, the data in the present study show no evidence for any significant degree of Na^+ and Si (H_4SiO_4) adsorption associated with surface precipitates (Na and Si congruency in Figs. 1c, 2c, 3c). Nonetheless, thick precipitation rinds (on the order of mm) can affect the outward flux of charged species (see Hellmann et al., 1989).

Precipitation and calculated chemical affinities

As noted in the Results section, there was often a discrepancy between the presence of Al-surface precipitates and calculated chemical affinities that were positive with respect to potential Al-bearing phases (see listed affinities in Figs. 1c, 2b,c, 3b,c, 5c). There are several reasons that can potentially explain these results. Perhaps the most obvious reason is related to analytical uncertitudes in the measured Al analyses. Uncertainty estimates for the calculated affinities were shown to be 1–3 kJ/mol (see Methods and Calculations section). These uncertainties are too low to account for the majority of the discrepancies. The second reason is related to inaccuracies in the Al hydrolysis and solubility constants used by the SUPCRT 92 thermodynamic database. This is not surprising, given the large differences in experimentally-determined Al phase solubilities in the literature (see e.g., Bourcier et al., 1993).

As seen in Fig. 6d,e, another explanation may be related to a phenomenon of localized solution supersaturation at sites of preferential dissolution (etch pits, grain boundaries, etc.) and bulk solution undersaturation. Mixing of small volumes of saturated or supersaturated fluids with a large volume of undersaturated fluid will result in an overall signal indicating fluid undersaturation with respect to potential precipitating phases (positive affinities). This type of a phenomenon indicates that affinities based on bulk fluid chemistry are of limited utility in describing localized precipitation processes on surfaces.

There is also the case where (metastable) surface precipitates are present, in the presence of solutions that are representative of stoichiometric dissolution conditions and are undersaturated with respect to Al phases. This behavior is best seen in Fig. 3c (and less clearly in Fig. 2a). The behavior of the Al rate curve suggests that during the initial stages of dissolution, the rapid release of Al resulted in the solution becoming locally supersaturated (note the positive affinities at the start of the expt.) with respect to an Al phase, resulting in precipitation. With continued dissolution, the subsequent decrease in the intrinsic rate of Al release from the albite structure eventually resulted in the solution becoming undersaturated, leading to the redissolution of the surface precipitate (shown by the rise in the Al rate curve). Eventually dissolution becomes congruent. The gradual asymptotic approach to congruency reflects the dissolution of precipitates remaining in isolated cracks and etch pits, which is what was observed by SEM.

A final explanation for positive affinities is the possible adsorption of aqueous Al onto the precipitated crystals. Figure 6c shows that the free surface area on the crystals that is theoretically available for adsorption reactions is quite considerable. Aluminum adsorption would suppress the measured Al concentrations in solution below that governed by the solubility of the Al phase in question, thereby resulting in positive affinities. Unfortunately, this explanation is not testable based on the present data.

CONCLUSIONS

The main emphasis of the present study was an analysis of the time evolution of the initial, pre-steady-state rates of release of Na, Al, and Si over a wide range of pH conditions at 100–300°C. The interpretation of the data yielded information on the preferential release of Na and Al (or Si), the formation, depths, and transport properties of leached layers, and the influence of Al surface precipitates. These data provide important evidence which show that reactions occurring within the leached layers influence the general dissolution process.

1) The time evolution of the rates of release of Na, Al, and Si generally showed the following characteristics: a very rapid initial increase, a monotonic decrease, an attainment of steady state. With respect to most of the dissolution conditions, the initial steady-state rates of release remained constant. However, at acid conditions and elevated temperatures, the initial steady-state rates of Na

and Si increased before new steady-state conditions were attained.

2) The sharp initial increases in the rates of release are due to ion exchange reactions ($H^+ \leftrightarrow Na^+$ at acid pH and $K^+ \leftrightarrow Na^+$ at basic pH) and to hydrolysis reactions of Si and Al occurring at the surface. Once readily detachable surface species are released into solution, the reaction front progresses into the structure.
3) The reaction front which advances into the structure is defined by the inward flux of aqueous species (H^+ or H_3O^+, Cl^-, H_2O, K^+, OH^-) which may participate in both ion exchange and hydrolysis reactions. The position of the reaction front theoretically corresponds to the maximum depth of preferential Na leaching (noting that ion exchange is always faster than hydrolysis). The inward and outward flux of species through the leached layers decrease with time as a consequence of the increasing distance of diffusional mass transfer. This decrease occurs until the fluxes equal the rate of retreat of the solid/solution interface. This feedback model, as described in the literature, limits the depths of preferential leaching. Even though the diffusion of reactants and products plays an important role in the development of leached layers, the overall rate of dissolution is governed by the rate of retreat of the solid/solution interface. This process is a function of the rates of bond hydrolysis and detachment, and not diffusion.
4) Once steady-state rates of release were achieved, the Na, Al, and Si rate curves (stoichiometrically normalized) were generally coincident, indicating congruent rates of release. At 100°C, however, the Al and Na rate curves were not coincident with the Si rate curves. This was attributed to the lower analytical accuracy of the Na and Al analyses, or possibly to the nonattainment of true steady-state conditions of dissolution.
5) At acid and neutral pH conditions (200° and 300°C), the Al release curves indicated the precipitation of an Al phase (boehmite (?) at 300°C) on the surface. The morphology of the Al precipitate crystals changed as a function of temperature. The chemical affinity calculations did not always correctly predict the supersaturation of the solutions with respect to Al phases. This was probably due to inaccuracies in both the Al analyses as well as in the thermodynamic database used. SEM images revealed the importance of sites of dissolution (etch pits) that led to localized areas of supersaturation and precipitation. These results show that precipitation reactions are not solely dependent on bulk solution thermodynamic saturation indices (affinity), but on the localized kinetics of precipitation, as well. SEM revealed that the precipitated crystals did not form an armoring carapace, which is the principle reason why the steady-state rates of Si release (i.e. overall dissolution rates) remained unaffected by the precipitation reactions.
6) At nearly all pH and temperature conditions, Na was preferentially released with respect to Al and Si. The maximum depths of preferential Na leaching (with respect to Si) were recorded at acid pH (1533 Å) and basic pH (1227 Å), while minima were recorded in the slightly acid to near-neutral pH range (25 Å). At the same conditions of dissolution, leaching depths may differ by an order of magnitude. This is a real phenomenon, and is most likely due to sample heterogeneities.
7) The depths of Na leaching did not increase dramatically with temperature. At pH 2.0, the average depths actually decreased with increasing temperature. This may be a function of the decreasing relative difference between the rates of ion exchange and Si hydrolysis as a function of increasing temperature. Nonetheless, more data are needed to establish an unambiguous relation between temperature and leaching depths.
8) Aluminum was preferentially released with respect to Si at acid and neutral pH conditions, even though exact depths could not be calculated at 200 and 300°C due to Al precipitation reactions. Where depths could be calculated, they were generally an order of magnitude less than those recorded for Na leaching. The difference in Na and Al leaching depths indicates that dissolution creates two distinct leached zones, one leached in both Na and Al, and one leached only in Na. The greatest recorded depths of Al leaching were at basic pH, minima were recorded at neutral pH. This result is important since significant Al-leached zones at basic pH conditions have not been previously observed in low temperature studies. Nonetheless, under mildly basic pH conditions, there was also evidence for Si preferential leaching with respect to Al, as well as congruent Al and Si release. At extreme basic pH conditions, however, Al was always (at 200 and 300°C) preferentially released.
9) The preferential release of Al at acid and neutral pH conditions is attributed to the predominance of positively charged $Al\text{-}OH_2^+$ groups with respect to neutral Si-OH groups within the leached layer. As the ratio of $Al\text{-}OH_2^+/Al\text{-}OH$ decreases with increasing pH, the degree of preferential leaching of Al should decrease; this is one possible reason why Al leaching depths are insignificant at neutral pH. Under mildly basic pH conditions, either Al or Si was preferentially released. First order calculations for the speciation of silanol and aluminol groups at temperature indicate that this occurs when both $Si\text{-}O^-$ and $Al\text{-}OH/Al\text{-}O^-$ groups predominate. However, it appears that when only $Si\text{-}O^-$ and $Al\text{-}O^-$ predominate (which occurs at extremely basic pH conditions), Al is always preferentially released. According to MO and ab initio results, $Al\text{-}O_{br}$ bonds are intrinsically more reactive than $Si\text{-}O_{br}$ bonds; this may be a decisive factor in causing Al to be preferentially released. However, to verify the above hypothesis, more experimental data, as well as calculations providing the exact speciation of silanol and aluminol groups at temperature would be required.
10) The interdependence between the initial rates of Al and Si release suggest that there is a weak but positive correlation between the preferential release of Al and the hydrolysis of Si. The reason for this is probably related to the different speciation of silanol and aluminol groups within the leached layers. The speciation of these groups is a major factor in determining their reactivity within leached layers.

11) There is evidence that leached layer depths are one factor which control the overall rate of dissolution, mainly by increasing the number of Al-O and Si-O bonds subject to attack by hydrolyzing molecules (H^+/H_3O^+ or OH^-). The dissolution rate vs. depth of Al leaching relationship (as revealed by the results on the plagioclase series; Fig. 15) also implies that deeper leached layers lead to increased rates of overall dissolution. The pH dependency of leached layer formation is probably a contributing factor to the pH dependency of overall feldspar dissolution rates. It is interesting to note that both Na-leached layer depths and overall feldspar dissolution rates roughly display a "U"-shaped relationship as a function of pH (Hellmann et al., 1990).
12) Based on the recorded fluxes and an assumed linear concentration gradient, the coefficients of diffusion for Na were calculated from Fick's first law. These were compared to the coefficients of diffusion (from the literature) for Na in albite and albite glass. At all temperatures, the experimentally-determined values for D_{Na} fell between those of albite and albite glass. This is a possible indication that the Na-leached layer is structurally more open than crystalline albite. The D_{Na} from this study also showed a pH dependence; there was a difference of up to several orders of magnitude for the D_{Na} at acid and basic pH with respect to neutral pH. This suggests that there is a greater degree of structural modification (i.e., openness) in leached layers formed under conditions (acid and basic pH) where the degree of preferential leaching is the most pronounced. The degree of structural openness of the leached layers influences both the rates of metal-oxygen hydrolysis as well as the subsequent detachment and outward diffusion of hydrolysis products.

Acknowledgments—I would like to thank Professor David A. Crerar of Princeton University for the 18 month loan of one of the flow systems. This study was an extension of feldspar dissolution kinetics research undertaken as a Ph.D. student with D. A. Crerar. David's life and scientific career were tragically cut short in September, 1994 by a fatal illness—to him this series of papers is dedicated.

The second flow system was carefully machined by C. Lurde at the Université Paul Sabatier, Toulouse. The following people's advice or assistance in the geochemistry lab at Toulouse was appreciated: G. Berger, J.-L. Dandurand, C. Monnin, B. Reynier, J. Schott. The use of an ICP at Societé Bioland in Toulouse is also gratefully acknowledged. Thanks are also due to M. Gugeon for the BET surface area measurements and C. Davidson (Princeton University) for the microprobe analyses of the Amelia albite. Assistance from B. Bourcier for providing access to a recently modified SUPCRT 92 database was appreciated. Thanks also go to J.-L. Hazemann for X-ray diffraction of the Al precipitates. Constructive comments by T. E. Burch, K. L. Nagy, and an anonymous reviewer greatly improved the quality of this paper.

Editorial handling: D. J. Rimstidt

REFERENCES

Aagaard P. and Helgeson H. C. (1982) Thermodynamic and kinetic constraints on reaction rates among minerals and aqueous solutions. I. Theoretical considerations. *Amer. J. Sci.* **282,** 237–285.

Allen L. H. and Matijevic E. (1969) Stability of colloidal silica I. Effect of simple electrolytes. *J. Colloid Interface Sci.* **31,** 287–296.

Allen L. H. and Matijevic E. (1970) Stability of colloidal silica II. Ion Exchange. *J. Colloid Interface Sci.* **33,** 420–429.

Allen L. H. and Matijevic E. (1971) Stability of colloidal silica III. Effect of hydrolyzable cations. *J. Colloid Interface Sci.* **35,** 66–76.

Amrhein C. and Suarez D. L. (1992) Some factors affecting the dissolution kinetics of anorthite at 25°C. *Geochim. Cosmochim. Acta* **56,** 1815–1826.

Berner R. A. and Holdren G. R., Jr. (1979) Mechanism of feldspar weathering: II. Observations of feldspars from soils. *Geochim. Cosmochim. Acta* **43,** 1173–1186.

Blum A. E. and Lasaga A. C. (1988) Role of surface speciation in the low-temperature dissolution of minerals. *Nature* **331,** 431–433.

Bourcier W. L., Knauss K. G., and Jackson K. J. (1993) Aluminum hydrolysis constants to 250°C from boehmite solubility measurements. *Geochim. Cosmochim. Acta* **57,** 747–762.

Brady P. V. (1994) Alumina surface chemistry at 25, 40, and 60°C. *Geochim. Cosmochim. Acta* **58,** 1213–1217.

Brady P. V. and Walther J. V. (1990) Kinetics of quartz dissolution at low temperatures. *Chem. Geol.* **82,** 253–264.

Brantley S. L. and Stillings L. (1995) Feldspar dissolution under acid conditions. *Amer. J. Sci.* (submitted).

Bunker B. C., Tallant D. R., Headley T. J., Turner G. L., and Kirkpatrick R. J. (1988) The structure of leached sodium silicate glass. *Phys. Chem. Glasses* **29,** 106–120.

Burch T. E., Nagy K. L., and Lasaga A. C. (1993) Free energy dependence of albite dissolution kinetics at 80°C and pH 8.8. *Chem. Geol.* **105,** 137–162.

Busenberg E. (1978) The products of the interaction of feldspars with aqueous solution at 25°C. *Geochim. Cosmochim. Acta* **42,** 1679–1686.

Busenberg E. and Clemency C. V. (1976) The dissolution kinetics of feldspars at 25°C and 1 atm CO_2 partial pressure. *Geochim. Cosmochim. Acta* **40,** 41–49.

Casey W. H., Westrich H. R., and Arnold G. W. (1988) Surface chemistry of labradorite feldspar reacted with aqueous solutions at pH = 2, 3, and 12. *Geochim. Cosmochim. Acta* **52,** 2795–2807.

Casey W. H., Westrich H. R., Arnold G. W., and Banfield J. F. (1989) The surface chemistry of dissolving labradorite feldspar. *Geochim. Cosmochim. Acta* **53,** 821–832.

Casey W. H., Westrich H. R., and Holdren G. R. (1991) Dissolution rates of plagioclase at pH = 2 and 3. *Amer. Mineral.* **76,** 211–217.

Casey W. H., Westrich H. R., Banfield J. F., Ferruzzi G., and Arnold G. W. (1993) Leaching and reconstruction at the surfaces of dissolving chain-silicate minerals. *Nature* **366,** 253–255.

Chou L. and Wollast R. (1984) Study of the weathering of albite at room temperature and pressure with a fluidized bed reactor. *Geochim. Cosmochim. Acta* **48,** 2205–2217.

Chou L. and Wollast R. (1985a) Steady-state kinetics and dissolution mechanisms of albite. *Amer. J. Sci.* **285,** 963–993.

Chou L. and Wollast R. (1985b) Study of the weathering of albite at room temperature and pressure with a fluidized bed reactor (Reply to a comment by R. A. Berner, G. R. Holdren Jr., and J. Schott). *Geochim. Cosmochim. Acta* **49,** 1659–1660.

Correns C. W. and von Engelhardt W. (1938) Neue Untersuchungen über die Verwitterung des Kalifeldspates. *Chem. Erde* **12,** 1–22.

de Jong B. H. W. S. and Brown G. E., Jr. (1980) Polymerization of silicate and aluminate tetrahedra in glasses, melts, and aqueous solutions: I. Electronic structure of $H_6Si_2O_7$, $H_6AlSiO_7^{1-}$, and $H_6Al_2O_7^{2-}$. *Geochim. Cosmochim. Acta* **44,** 491–511.

Dibble W. E., Jr., and Tiller W. A. (1981) Non-equilibrium water/rock interactions: I. Model for interface-controlled reactions. *Geochim. Cosmochim. Acta* **45,** 79–92.

Dugger D. L., Stanton J. H., Irby B. N., McConnell B. L., Cummings W. W., and Maatman R. W. (1964) The exchange of twenty metal ions with the weakly acidic silanol group of silica gel. *J. Phys. Chem.* **68,** 757–760.

Fung P. C., Bird G. W., McIntyre N. S., Sanipelli G. G., and Lopata V. J. (1980) Aspects of feldspar dissolution. *Nuclear Technology* **51,** 188–196.

Garrels R. M. and Howard P. (1957) Reactions of feldspar and mica with water at low temperature and pressure. In *Proc. 6th Natl. Conf. on Clays and Clay Minerals,* pp. 68–88. Pergamon Press.

Geisinger K. L., Gibbs G. V., and Navrotsky A. (1985) A molecular orbital study of bond length and angle variations in framework structures. *Phys. Chem. Minerals* **11,** 266–283.

Gommes W. P. and Dekeyser W. (1976) Factors influencing the reactivity of solids. In *Reactivity of Solids* (ed. N. B. Hannay); *Treatise on Solid State Chemistry 4,* pp. 61–113. Plenum Press.

Harlow G. E. and Brown G. E., Jr. (1980) Low albite: an X-ray and neutron diffraction study. *Amer. Mineral.* **65,** 986–995.

Helgeson H. C. (1971) Kinetics of mass transfer among silicates and aqueous solutions. *Geochim. Cosmochim. Acta* **35,** 421–469.

Helgeson H. C. (1972) Kinetics of mass transfer among silicates and aqueous solutions: correction and clarification. *Geochim. Cosmochim. Acta* **36,** 1067–1070.

Hellmann R. (1994) The albite-water system: Part I. The kinetics of dissolution as a function of pH at 100, 200, and 300°C. *Geochim. Cosmochim. Acta* **58,** 595–611.

Hellmann R., Crerar D. A., and Zhang R. (1989) Albite feldspar hydrolysis to 300°C. In *Reactivity of Solids: Proceedings of the 11th Symposium* (ed. M. S. Whittingham et al.), Part I, pp. 314–329. North Holland.

Hellmann R., Eggleston C. M., Hochella M. F., Jr., and Crerar D. A. (1990) The formation of leached layers on albite surfaces during dissolution under hydrothermal conditions. *Geochim. Cosmochim. Acta* **54,** 1267–1281.

Hellmann R., Dran J.-C., and Della Mea G. (1995) The albite-water system: Part III. Characterization of leached layers formed at 300°C using MeV ion beam techniques and HRTEM. *Geochim. Cosmochim. Acta* (in prep.).

Hochella M. F., Jr., Ponader H. B., Turner A. M., and Harris D. W. (1988) The complexity of mineral dissolution as viewed by high resolution scanning Auger microscopy: Labradorite under hydrothermal conditions. *Geochim. Cosmochim. Acta* **52,** 385–394.

Hohl H., and Stumm W. (1976) Interaction of Pb^{+2} with hydrous γ-Al_2O_3. *J. Colloid Interface Sci.* **55,** 281–288.

Holdren G. R., Jr., and Adams J. E. (1982) Parabolic dissolution kinetics of silicate minerals: An artifact of nonequilibrium precipitation processes? *Geology* **10,** 186–190.

Holdren G. R., Jr., and Berner R. A. (1979) Mechanism of feldspar weathering: I. Experimental studies. *Geochim. Cosmochim. Acta* **43,** 1161–1171.

Holdren G. R. Jr., and Speyer P. M. (1985) Reaction rate-surface area relationships during the early stages of weathering: I. Initial observations. *Geochim. Cosmochim. Acta* **49,** 675–681.

Iler R. K. (1973) Effect of adsorbed alumina on the solubility of amorphous silica in water. *J. Colloid Interface Sci.* **43,** 399–408.

Iler R. K. (1979) *The Chemistry of Silica.* Wiley.

Jambon A. and Carron J. P. (1976) Diffusion of Na, K, Rb, and Cs in glasses of albite and orthoclase composition. *Geochim. Cosmochim. Acta* **40,** 897–903.

Johnson J. W., Oelkers E. H., and Helgeson H. C. (1992) SUPCRT 92: A software package for calculating the standard molal thermodynamic properties of minerals, gases, aqueous species, and reactions from 1 to 5000 bar and 0 to 1000°C. *Comput. Geosci.* **18,** 899–947.

Kasper R. B. (1975) Cation and oxygen diffusion in albite. Ph.D. thesis, Brown University.

Kummert R. and Stumm W. (1980) Surface complexation of organic acids on hydrous γ-Al_2O_3. *J. Colloid Interface Sci.* **75,** 373–385.

Lagache M. (1965) Contribution à l'étude de l'altération des feldspaths, dans l'eau, entre 100 et 200°C, sous diverses pressions de CO_2, et application à la synthèse des minéraux argileux. *Bull. Soc. franç. Minér. Crist.* **88,** 223–253.

Lasaga A. C. (1981) Rate laws of chemical reactions. In *Kinetics of Geochemical Processes* (ed. A. C. Lasaga and R. J. Kirkpatrick); *Reviews in Mineralogy 8,* pp. 1–68. Mineral. Soc. Amer.

Luce R. W., Bartlett R. W., and Parks G. A. (1972) Dissolution kinetics of magnesium silicates. *Geochim. Cosmochim. Acta* **36,** 35–50.

Machesky M. L. and Jacobs P. F. (1991) Titration calorimetry of aqueous alumina suspensions: Part II. Discussion of enthalpy changes with pH and ionic strength. *Colloids and Surfaces* **53,** 315–328.

Matijevic E., Mangravite F. J., Jr., and Cassel E. A. (1971) Stability of colloidal silica: IV. The silica-alumina system. *J. Colloid Interface Sci.* **35,** 560–568.

Marshall W. L. and Franck E. U. (1981) Ion product of water substance, 0–1000°C, 1–10000 bars New international formulation and its background. *J. Phys. Chem. Ref. Data* **10,** 295–304.

Muir I. J. and Nesbitt H. W. (1991) Effects of aqueous cations on the dissolution of labradorite feldspar. *Geochim. Cosmochim. Acta* **55,** 3181–3189.

Muir I. J., Bancroft G. M., and Nesbitt H. W. (1989) Characteristics of altered labradorite surfaces by SIMS and XPS. *Geochim. Cosmochim. Acta* **53,** 1235–1241.

Muir I. J., Bancroft G. M., Shotyk W., and Nesbitt H. W. (1990) A SIMS and XPS study of dissolving plagioclase. *Geochim. Cosmochim. Acta* **54,** 2247–2256.

Oelkers E. H., Schott J., and Devidal J.-L. (1994) The effect of aluminum, pH, and chemical affinity on the rates of aluminosilicate dissolution rates. *Geochim. Cosmochim. Acta* **58,** 2011–2024.

Pačes T. (1973) Steady-state kinetics and equilibrium between ground water and granitic rock. *Geochim. Cosmochim. Acta* **37,** 2641–2663.

Parks G. A. (1965) The isoelectric points of solid oxides, solid hydroxides, and aqueous hydroxo complex systems. *Chem. Rev.* **65,** 177–198.

Parks G. A. (1990) Surface energy and adsorption at mineral-water interfaces: An introduction. In *Mineral-Water Interface Geochemistry* (ed. M. F. Hochella, Jr., and A. F. White); *Reviews in Mineralogy 23,* pp. 133–175. Mineral. Soc. Amer.

Pederson L. R., Baer D. R., McVay G. L., and Engelhard M. H. (1986) Reaction of soda-lime silicate glass in isotopically labelled water. *J. Non-Crys. Solids* **86,** 369–380.

Petit J.-C., Della Mea G., Dran J.-C., Schott J., and Berner R. A. (1987) Mechanism of diopside dissolution from hydrogen depth profiling. *Nature* **325,** 705–707.

Petit J.-C., Della Mea G., Dran J.-C., Magonthier M.-C., Mando P. A., and Paccagnella A. (1990) Hydrated layer formation during dissolution of complex silicate glasses and minerals. *Geochim. Cosmochim. Acta* **54,** 1941–1955.

Petrovich R. (1981a) Kinetics of dissolution of mechanically comminuted rock-forming oxides and silicates: I. Deformation and dissolution of quartz under laboratory conditions. *Geochim. Cosmochim. Acta* **45,** 1665–1674.

Petrovich R. (1981b) Kinetics of dissolution of mechanically comminuted rock-forming oxides and silicates: II. Deformation and dissolution of oxides and silicates in the laboratory and at the Earth's surface. *Geochim. Cosmochim. Acta* **45,** 1675–1686.

Petrović R., Berner R. A., and Goldhaber M. B. (1976) Rate control in dissolution of alkali feldspars. I. Study of residual grains by X-ray photoelectron spectroscopy. *Geochim. Cosmochim. Acta* **40,** 537–548.

Pokrovskii V. A. and Helgeson H. C. (1995) Thermodynamic properties of aqueous species and the solubilities of minerals at high pressures and temperatures: the system Al_2O_3-H_2O-NaCl. *Amer. J. Sci.* **295.**

Robie R. A., Hemingway B. S., and Fisher J. R. (1984) Thermodynamic Properties of Minerals and Related Substances at 298.15 K and 1 Bar (10^5 Pascals) Pressure and at Higher Temperatures. U.S.G.S. Bull. 1432.

Rose N. M. (1991) Dissolution rates of prehnite, epidote, and albite. *Geochim. Cosmochim. Acta* **55,** 3273–3286.

Schindler P. W. and Kamber H. R. (1968) Die Acidität von Silanolgruppen. *Helv. Chim. Acta* **51,** 1781–1786.

Schott J. (1990) Modeling of the dissolution of strained and unstrained multiple oxides: the surface speciation approach. In *Aquatic Chemical Kinetics* (ed. W. Stumm), pp. 337–365. Wiley.

Schweda P. (1990) Kinetics and mechanisms of alkali feldspar dissolution at low temperatures. Doctoral thesis, Stockholms Universitets Institution för Geologi och Geokemi.

Shotyk W. and Nesbitt H. W. (1992) Incongruent and congruent dissolution of plagioclase feldspar: effect of feldspar composition and ligand complexation. *Geoderma* **55,** 55–78.

Sigg L. (1973) Untersuchungen über Protolyse und Komplexbildung mit zweiwertigen Kationen von Silikageloberflächen. M. Sc. thesis, University of Bern.

Smith J. V. and Brown W. L. (1988) *1. Crystal Structures, Physical, Chemical and Microtextural Properties.* Springer-Verlag.

Stillings L. L. and Brantley S. L. (1995) Feldspar dissolution at 25°C and pH 3: Reaction stoichiometry and the effect of ionic strength. *Geochim. Cosmochim. Acta* **59,** 1483–1496.

Taylor M. and Brown G. E., Jr. (1979) Structure of mineral glasses: I. The feldspar glasses $NaAlSi_3O_8$, $KAlSi_3O_8$, $CaAl_2Si_2O_8$. *Geochim. Cosmochim. Acta* **43,** 61–75.

Tewari P. H. and McLean A. W. (1972) Temperature dependence of point of zero charge of alumina and magnetite. *J. Colloid Interface Sci.* **40,** 267–272.

Tsuzuki Y. and Suzuki K. (1980) Experimental study of the alteration process of labradorite in acid hydrothermal solutions. *Geochim. Cosmochim. Acta* **44,** 673–683.

Velbel M. A. (1993) Constancy of silicate-mineral weathering-rate ratios between natural and experimental weathering: implications for hydrologic control of differences in absolute rates. *Chem. Geol.* **105,** 89–99.

Vydra F. and Galba J. (1967) Sorption von Metallkomplexen an Silicagel III. Sorption von Hydrolysenprodukten des Th^{4+}, Fe^{3+}, Al^{3+} und Cr^{3+}. *Collec. Czechoslovak Chem. Comm.* **32,** 3530–3536.

Welch S. A. and Ullman W. J. (1993) The effect of organic acids on plagioclase dissolution rates and stoichiometry. *Geochim. Cosmochim. Acta* **57,** 2725–2736.

Wolery T. J. (1992) *EQ3NR, A Computer Program for Geochemical Aqueous Speciation-Solubility Calculations: Theoretical Manual, User's Guide, and Related Documentation (Version 7.0).* Lawrence Livermore Natl. Lab. UCRL-MA-110662 PT III.

Wolery T. J. and Daveler S. A. (1992) *EQ6, A Computer Program for Reaction Path Modeling of Aqueous Geochemical Systems: Theoretical Manual, User's Guide, and Related Documentation (Version 7.0).* Lawrence Livermore Natl. Lab. UCRL-MA-110662 PT IV.

Wollast R. (1967) Kinetics of the alteration of K-feldspar in buffered solutions at low temperature. *Geochim. Cosmochim. Acta* **31,** 635–648.

Xiao Y. and Lasaga A. C. (1994) Ab initio quantum mechanical studies of the kinetics and mechanisms of silicate dissolution: H^+ (H_3O^+) catalysis. *Geochim. Cosmochim. Acta* **58,** 5379–5400.